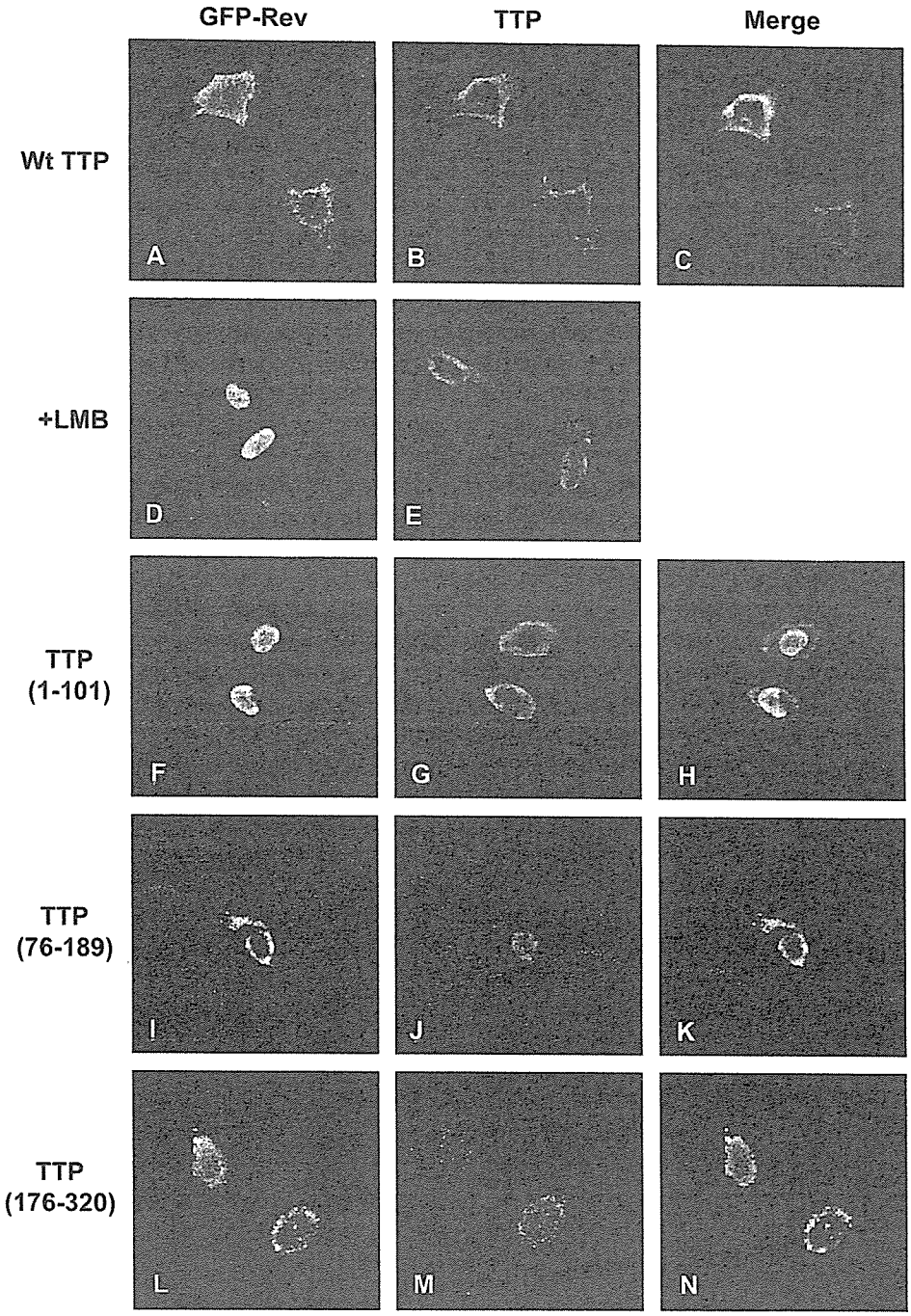

Fig. 6. Effects of TTP on the subcellular localization of Rev. HeLa cells (2.5×10^4 per well in a 12-well dish) were cotransfected with an expression plasmid for GFP-Rev (0.1 μg) and 0.3 μg of pchTTPwt (A, B, C), pcD1–101 (F, G, H), pcD76–189 (I, J, K) or pcD176–320 (L, M, N). Similarly, HeLa cells were transfected with 0.4 μg of GFP-Rev (D) or pchTTPwt (E). The cells were incubated for 90 min with leptomycin B (5 ng/ml) before analysis (D, E). The subcellular localization of GFP-Rev was monitored by GFP fluorescence (A, D, F, I, L). Immunofluorescent signals of wild-type TTP (B, E) or the mutant 1–101 (G), 76–189 (J), and 176–320 TTP (M) were examined by anti-Xpress antibody. Merged images of Rev and wild-type and mutant TTP are shown in C, H, K, and N.

marker protein, green fluorescent protein (GFP-Rev) and wild-type or the mutant TTP were co-expressed in HeLa cells (Fig. 6A–C). Both GFP-Rev and wild-type TTP were found to be localized predominantly in the cytoplasm and to a lesser extent in the nucleus and nucleolus. Singly expressed GFP-Rev or wild-type TTP showed the similar localization (data not shown). Rev and TTP are known to shuttle between the nucleolus and the cytoplasm [28]. Treatment of the cells with leptomycin B, which inhibits the CRM1-mediated nuclear export [28], resulted in the accumulation of GFP-Rev or wild-type TTP in the nucleus and nucleolus (Fig. 6D,E).

GFP-Rev was restricted to the nucleus and nucleolus in the cells expressing the TTP mutant 1–101, which itself was largely restricted to the cytoplasm (Fig. 6F–H). Both the TTP

mutant 76–189 and 176–320 did not affect on the localization of GFP-Rev (Fig. 6I–N). As has been reported previously [28], the 76–189 mutant localized in the nucleus (Fig. 6J).

4. Discussion

In the present study we have demonstrated that TTP inhibits HIV-1 production by promoting multiple splicing by direct binding to AU-rich sequences. Because TTP increased luciferase activity of NL-luc virus, which is derived from multiple spliced transcripts, inhibition of HIV-1 production was not due to nonspecific damage of the cells induced by overexpression of TTP, but due to a specific suppression by TTP binding to HIV-1 RNA.

Although the TTP mutant 1–101 lacking NLS could suppress the production derived from un-, single-spliced RNA, it did not increase the product of multiple-spliced RNA. Among the wild-type TTP and its mutants, the 1–101 mutant exclusively suppressed nuclear export of Rev similarly to leptomycin B. It is suggested that the NES sequence of the 1–101 mutant plays an important role in suppression of nuclear export of Rev. Because the 1–101 mutant is not capable of binding with RNA, marked suppression of CAT expression by the 1–101 mutant (Fig. 4C) seems to be mainly dependent on competition with Rev for binding to CRM1 which shuttles between cytoplasm and nucleus. In contrast, wild-type TTP, which directly binds to AU-rich sequence of HIV-1 RNAs, did not affect subcellular localization of Rev and increased the production of multiple-spliced RNA. Although the 76–189 mutant, which predominantly localizes in the nucleus (Fig. 6), has RNA binding activity, this mutant could not enhance the splicing HIV-1 RNA, suggesting that the nuclear localization might be related to abrogation of splicing HIV-1 RNA.

Turnover of mRNA for certain cytokines containing an ARE (AUUUA) in their 3′-untranslated region is regulated by *cis* elements and *trans*-acting factors, TTP [10]. Although sequences of HIV-1 do not contain ARE, as we found that ARE of GM-CSF mRNA was cleaved between U and A residues we expected that TTP might destabilize HIV-1 RNA, which contains AU-rich sequences [2]. However, TTP did not significantly affect HIV-1 RNA stability (data not shown). This result may be explained by the following reasons. Firstly, HIV-1 AU-rich sequences were not so effectively cleaved by TTP as ARE in GM-CSF mRNA, so we could not obtain the significant decrease of HIV-1 RNA using our assay system even in the presence of TTP. Secondly, actinomycin D in the assay system could not completely suppress the transcription of HIV-1 RNA. Other experiments would be required to demonstrate destabilization of HIV-1 RNA by TTP.

Given that TTP is exclusively expressed in activated $CD4^+$ T cells, which are targets of HIV-1, TTP might inhibit virion production in these cells and thereby inhibit the presentation of viral antigens by MHC class I molecules on the cell surface, thus contributing to persistence of an HIV-1 reservoir in T cells. The resulting inactivated cells harboring a silent HIV-1 genome might be subsequently reactivated by various stimuli and produce HIV-1 virions.

ZAP, a family of RNA binding proteins carrying CCCH-type zinc fingers, also inhibit retroviral RNA production [29]. Zinc fingers of TTP and ZAP may play an important role in nuclear retention or decay of genomic RNA with a different mechanism as RNA interference. Further studies are required to reveal the precise mechanism by which TTP affects HIV-1 RNA trafficking mediated by Rev [30].

Acknowledgments

We thank Dr. B.R. Cullen (Duke University) for providing pCMV128, pDM128/CTE and Dr. K. Ikuta (Osaka University) for the gifts of U1 cells and antibodies to Nef and p24. We also thank Dr. H. Shida (Hokkaido University) for providing pSRαRev. This work was supported in part by grants from the Ministry of Education, Science, Technology, Sports, and Culture of Japan, the Ministry of Health, Labor, and Welfare of Japan, the Japan Human Science Foundation, and the Japanese Foundation for AIDS Prevention.

References

[1] A.W. Cochrane, K.S. Jones, S. Beidas, P.J. Dillon, A.M. Skalka, C.A. Rosen, Identification and characterization of intragenic sequences which repress human immunodeficiency virus structural gene expression, J. Virol. 65 (1991) 5305–5313.

[2] W. Tan, S. Schwartz, The Rev protein of human immunodeficiency virus type 1 counteracts the effect of an AU-rich negative element in the human papillomavirus type 1 late 3′ untranslated region, J.Virol. 69 (1995) 2932–2945.

[3] M. Graf, A. Bojak, L. Deml, K. Bieler, H. Wolf, R. Wagner, Concerted action of multiple cis-acting sequences is required for Rev dependence of late human immunodeficiency virus type 1 gene expression, J.Virol. 74 (2000) 10822–10826.

[4] A.S. Zolotukhin, A. Valentin, G.N. Pavlakis, B.K. Felber, Continuous propagation of RRE(-) and Rev(-)RRE(-) human immunodeficiency virus type 1 molecular clones containing a cis-acting element of simian retrovirus type 1 in human peripheral blood lymphocytes, J. Virol. 68 (1994) 7944–7952.

[5] H. Takahashi, H. Sawa, H. Hasegawa, T. Sata, W.W. Hall, K. Nagashima, T. Kurata, Reconstitution of cleavage of human immunodeficiency virus type-1 (HIV-1) RNAs, Biochem. Biophys. Res. Commun. 293 (2002) 1084–1091.

[6] J.S. McDougal, A. Mawle, S.P. Cort, J.K. Nicholson, G.D. Cross, J.A. Scheppler-Campbell, D. Hicks, J. Sligh, Cellular tropism of the human retrovirus HTLV-III/LAV.I. Role of T cell activation and expression of the T4 antigen, J. Immunol. 135 (1985) 3151–3162.

[7] J.A. Zack, A.M. Haislip, P. Krogstad, I.S. Chen, Incompletely reverse-transcribed human immunodeficiency virus type 1 genomes in quiescent cells can function as intermediates in the retroviral life cycle, J. Virol. 66 (1992) 1717–1725.

[8] A. Clark, Post-transcriptional regulation of pro-inflammatory gene expression, Arthritis Res. 2 (2000) 172–174.

[9] A. Bevilacqua, M.C. Ceriani, S. Capaccioli, A. Nicolin, Post-transcriptional regulation of gene expression by degradation of messenger RNAs, J. Cell Physiol. 195 (2003) 356–372.

[10] N. Xu, C.Y. Chen, A.B. Shyu, Modulation of the fate of cytoplasmic mRNA by AU-rich elements: key sequence features controlling mRNA deadenylation and decay, Mol. Cell. Biol. 17 (1997) 4611–4621.

[11] T.M. Folks, J. Justement, A. Kinter, C.A. Dinarello, A.S. Fauci, Cytokine-induced expression of HIV-1 in a chronically infected promonocyte cell line, Science 238 (1987) 800–802.
[12] M. Tobiume, M. Takahoko, T. Yamada, M. Tatsumi, A. Iwamoto, M. Matsuda, Inefficient enhancement of viral infectivity and CD4 down-regulation by human immunodeficiency virus type 1 Nef from Japanese long-term nonprogressors, J. Virol. 76 (2002) 5959–5965.
[13] Y. Hakata, M. Yamada, H. Shida, A multifunctional domain in human CRM1 (exportin 1) mediates RanBP3 binding and multimerization of human T-cell leukemia virus type 1 Rex protein, Mol. Cell. Biol. 23 (2003) 8751–8761.
[14] A. Adachi, H.E. Gendelman, S. Koenig, T. Folks, R. Willey, A. Rabson, M.A. Martin, Production of acquired immunodeficiency syndrome-associated retrovirus in human and nonhuman cells transfected with an infectious molecular clone, J. Virol. 59 (1986) 284–291.
[15] K. Tokunaga, A. Kojima, T. Kurata, K. Ikuta, H. Akari, A.H. Koyama, M. Kawamura, R. Inubushi, R. Shimano, A. Adachi, Enhancement of human immunodeficiency virus type 1 infectivity by Nef is producer cell-dependent, J. Gen. Virol. 79 (Pt 10) (1998) 2447–2453.
[16] R. Shibata, H. Sakai, M. Kawamura, K. Tokunaga, A. Adachi, Early replication block of human immunodeficiency virus type 1 in monkey cells, J. Gen. Virol. 76 (Pt 11) (1995) 2723–2730.
[17] T.M. Ross, B.R. Cullen, The ability of HIV type 1 to use CCR-3 as a coreceptor is controlled by envelope V1/V2 sequences acting in conjunction with a CCR-5 tropic V3 loop, Proc. Natl. Acad. Sci. USA 95 (1998) 7682–7686.
[18] R.A. Fouchier, B.E. Meyer, J.H. Simon, U. Fischer, M.H. Malim, HIV-1 infection of non-dividing cells: evidence that the amino-terminal basic region of the viral matrix protein is important for Gag processing but not for post-entry nuclear import, EMBO J 16 (1997) 4531–4539.
[19] G.A. Taylor, W.S. Lai, R.J. Oakey, M.F. Seldin, T.B. Shows, R.L. Eddy Jr., P.J. Blackshear, The human TTP protein: sequence, alignment with related proteins, and chromosomal localization of the mouse and human genes, Nucleic Acids Res. 19 (1991) 3454.
[20] Z. Tsuchihashi, P.O. Brown, DNA strand exchange and selective DNA annealing promoted by the human immunodeficiency virus type 1 nucleocapsid protein, J. Virol. 68 (1994) 5863–5870.
[21] D.P. Bednarik, T.M. Folks, Mechanisms of HIV-1 latency, AIDS 6 (1992) 3–16.
[22] M. Tobiume, K. Fujinaga, M. Kameoka, T. Kimura, T. Nakaya, T. Yamada, K. Ikuta, Dependence on host cell cycle for activation of human immunodeficiency virus type 1 gene expression from latency, J. Gen. Virol. 79 (Pt 6) (1998) 1363–1371.
[23] A.M. Fairhurst, J.E. Connolly, K.A. Hintz, N.J. Goulding, A.J. Rassias, M.P. Yeager, W. Rigby, P.K. Wallace, Regulation and localization of endogenous human tristetraprolin, Arthritis Res. Ther. 5 (2003) R214–R225.
[24] K. Tokunaga, M.L. Greenberg, M.A. Morse, R.I. Cumming, H.K. Lyerly, B.R. Cullen, Molecular basis for cell tropism of CXCR4-dependent human immunodeficiency virus type 1 isolates, J. Virol. 75 (2001) 6776–6785.
[25] Y. Luo, H. Yu, B.M. Peterlin, Cellular protein modulates effects of human immunodeficiency virus type 1 Rev, J. Virol. 68 (1994) 3850–3856.
[26] I. Mikaelian, M. Krieg, M.J. Gait, J. Karn, Interactions of INS (CRS) elements and the splicing machinery regulate the production of Rev-responsive mRNAs, J. Mol. Biol. 257 (1996) 246–264.
[27] K.S. Cook, G.J. Fisk, J. Hauber, N. Usman, T.J. Daly, J.R. Rusche, Characterization of HIV-1 REV protein: binding stoichiometry and minimal RNA substrate, Nucleic Acids Res. 19 (1991) 1577–1583.
[28] T. Murata, Y. Yoshino, N. Morita, N. Kaneda, Identification of nuclear import and export signals within the structure of the zinc finger protein TIS11, Biochem. Biophys. Res. Commun. 293 (2002) 1242–1247.
[29] G. Gao, X. Guo, S.P. Goff, Inhibition of retroviral RNA production by ZAP, a CCCH-type zinc finger protein, Science 297 (2002) 1703–1706.
[30] N. Sanchez-Velar, E.B. Udofia, Z. Yu, M.L. Zapp, hRIP, a cellular cofactor for Rev function, promotes release of HIV RNAs from the perinuclear region, Genes Dev. 18 (2004) 23–34.

Antiviral Chemistry & Chemotherapy 17:167–174

Rapid propagation of low-fitness drug-resistant mutants of human immunodeficiency virus type 1 by a streptococcal metabolite sparsomycin

Kosuke Miyauchi, Jun Komano*, Lay Myint, Yuko Futahashi, Emiko Urano, Zene Matsuda, Tomoko Chiba, Hideka Miura, Wataru Sugiura and Naoki Yamamoto

AIDS Research Center, National Institute of Infectious Diseases, Toyama, Shinjuku, Tokyo, Japan

*Corresponding author: Tel: +81 3 5285 1111; Fax: +81 3 5285 5037; E-mail: ajkomano@nih.go.jp

Here we report that sparsomycin, a streptococcal metabolite, enhances the replication of HIV-1 in multiple human T cell lines at a concentration of 400 nM. In addition to wild-type HIV-1, sparsomycin also accelerated the replication of low-fitness, drug-resistant mutants carrying either D30N or L90M within HIV-1 protease, which are frequently found mutations in HIV-1-infected patients on highly active antiretroviral therapy (HAART). Of particular interest was that replication enhancement appeared profound when HIV-1 such as the L90M-carrying mutant displayed relatively slower replication kinetics. The presence of sparsomycin did not immediately select the fast-replicating HIV-1 mutants in culture. In addition, sparsomycin did not alter the 50% inhibitory concentration (IC_{50}) of antiretroviral drugs directed against HIV-1 including nucleoside reverse transcriptase inhibitors (lamivudine and stavudine), non-nucleoside reverse transcriptase inhibitor (nevirapine) and protease inhibitors (nelfinavir, amprenavir and indinavir). The IC_{50}s of both zidovudine and lopinavir against multidrug resistant HIV-1 in the presence of sparsomycin were similar to those in the absence of sparsomycin. The frameshift reporter assay and Western blot analysis revealed that the replication-boosting effect was partly due to the sparsomycin's ability to increase the −1 frameshift efficiency required to produce the *Gag–Pol* transcript. In conclusion, the use of sparsomycin should be able to facilitate the drug resistance profiling of the clinical isolates and the study on the low-fitness viruses.

Keywords: drug resistant mutants, enhancement of replication, HIV-1, low-fitness mutants, sparsomycin

Introduction

Highly active antiretroviral therapy (HAART) has been successful in controlling the progression of AIDS caused by HIV-1. However, HAART has accelerated the emergence and spread of multidrug-resistant HIV-1. Once drug-resistant HIV-1 occurs in a HIV-1-infected patient, the success rate of HAART drops substantially. Resistance testing has been shown to be valuable to optimize HAART against HIV-1 infection (Hirsch *et al.*, 2000; Rodriguez-Rosado *et al.*, 1999). Profiling drug resistance might be necessary even before the initiation of HAART because of the spread of drug-resistant HIV-1 (Boden *et al.*, 1999; Gehringer *et al.*, 2000; Yerly *et al.*, 1999).

Genotypic and phenotypic resistance testing are the two major ways to determine the drug resistance of clinical HIV-1 isolates. For genotyping, the HIV-1 genome isolated from the infected individuals is sequenced. This HIV-1 genome is than cross-referenced with a database and we are able to predict the drug resistance profile of HIV-1. However, it is impossible to predict the phenotype when we encounter a combination of mutations that has never been documented. This may raise a concern when a new drug is released in the market. Another problem in the genotyping is the presence of genotype-phenotype discordance (Parkin *et al.*, 2003; Sarmati *et al.*, 2002).

Alternatively, for the phenotypic resistance testing, the drug resistance profiles are measured by many biological/virological assay systems (Hertogs *et al.*, 1998; Iga *et al.*, 2002; Jarmy *et al.*, 2001; Kellam & Larder, 1994; Menzo *et al.*, 2000; Walter *et al.*, 1999). Phenotypic resistance testing is powerful because the diagnosis is based on experimental observations. Among the systems, ones that depend on the multi-round HIV-1 replication seemed to provide the best drug resistance data reflecting the *in vivo* condition. However, many drug-resistant mutants have lower replication capabilities than wild-type (wt) HIV-1, which makes the phenotypic resistance testing difficult and time-consuming. In order to overcome these problems, it would be useful to develop a technique to make HIV-1

replicate faster without altering the effectiveness of antiretroviral compounds.

During our search for an inhibitor of HIV-1 replication, we found sparsomycin, a metabolite from *Streptomyces sparsogenes*, which reproducibly enhanced the replication of HIV-1. Therefore, we tested whether sparsomycin merits phenotypic drug resistance profiling studies on low-fitness HIV-1 isolates.

Materials and methods

Cells and viruses

Human embryonic kidney (HEK) 293T cells were maintained in Dulbecco's modified Eagle's medium (Sigma-Aldrich, Tokyo, Japan) supplemented with 10% fetal bovine serum (FBS; Hyclone, Logan, UT, USA), penicillin and streptomycin (Invitrogen, Carlsbad, CA, USA). H9, Jurkat, SupT1 and HPB-Ma cells were maintained in RPMI1640 (Sigma-Aldrich) supplemented with 10% FBS, penicillin and streptomycin. All the cell lines were incubated at 37°C in a humidified 5% CO_2 atmosphere. As previously described, HIV-1 (HXB2) was produced by transfecting proviral DNA into 293T cells and collecting the culture medium 3 days post-transfection (Komano *et al.*, 2004). The replication-incompetent HIV-1 (HXB2 Δ*vpr*, Δ*rev*, Δ*env*, Δ*nef*) was produced by transfecting the proviral DNA carrying renilla luciferase with the *nef* open reading frame into 293T cells, along with the expression plasmid for *env*, *tat*, *rev* and *nef* (pIIIex) as described previously in Komano *et al.* (2004). As previously described, the D30N, L90M, and D25N protease mutants of HIV-1 were generated by the site-directed mutagenesis (Sugiura *et al.*, 2002). The multidrug-resistant HIV-1 DR3577 was a clinical isolate from a patient on HAART in which reverse transciptase carried the following mutations M41L, D67N, K70R, V75M, K101Q, T215F and K219Q and protease carried the following mutations L10I, K20R, M36I, M46I, L63P, A71V, V82T, N88S and L90M. For the generation of replication-incompetent murine leukaemia virus (MLV) vector expressing firefly luciferase, pCMMP luciferase was transfecting into 293T cells along with *gag/pol* and VSV-G expressing plasmids as described previously (Komano *et al.*, 2004).

Chemical compound

Sparsomycin was either purchased from Sigma-Aldrich (cat. S1667) or obtained from Dr Nakajima (Toyama Prefectural University, Toyama, Japan). Sparsomycin was dissolved in 2mM dimethyl sulphoxide and stored at −20°C until use.

Monitoring HIV-1 replication

For HIV-1 infection, 1×10^6 cells were incubated with the culture supernatant containing approximately 10 ng of p24. Alternatively, wt HIV-1, or D30N and L90M mutants were introduced into cells either by electroporation or DEAE-dextran-mediated protocol as previously described (Matsuda *et al.*, 1993; Miyauchi *et al.*, 2005). The culture supernatants were collected everytime the infected cells were split until they ceased to proliferate. The amount of p24 antigen of HIV-1 in the culture supernatants was quantified by using Retro TEK p24 antigen ELISA kit according to the manufacturer's protocol (Zepto Metrix, Buffalo, NY, USA). The signal was detected by Vmax ELISA reader (Molecular Devices, Palo Alto, CA, USA).

Determining 50% inhibitory concentrations (IC_{50})

IC_{50} was calculated by using a reporter cell line, MARBLE, developed by Sugiura *et al.* (personal communication). In brief, a clone of HPB-Ma carrying the long terminal repeat (LTR)-driven firefly luciferase cassette integrated in its genome was infected with HIV-1 and incubated in the presence of varying concentrations of antiretroviral compounds for a week. The cells were then lysed to measure the firefly luciferase activity, which represented the propagation of HIV-1 in culture. The firefly luciferase activity was normalized by constitutively-expressed renilla luciferase activity. The dual luciferase assay was performed according to the manufacturer's protocol (Promega, Madison, WI, USA). Chemiluminescence was detected by Lmax (Molecular Devices).

Reporter assay

The −1 frameshift reporters, pLuc (−1) and pLuc (0), were kindly provided by Dr Brakier-Gingras (Dulude *et al.*, 2002). The renilla luciferase expression vector phRL/CMV was purchased from Promega. pLTR Luc encoded GFP-luciferase under the regulation of HIV-1's LTR promoter (Komano *et al.*, 2004). pLTRΔnefLuc encoded renilla luciferase by substituting *nef* in the proviral context of HXB2 (Komano *et al.*, 2004). Plasmids were transfected into 293T cells by Lipofectamine 2000 plus reagent in accordance with the manufacturers' protocol (Invitrogen). For the detection of luciferase activities, the dual glo luciferase assay was performed at 2–3 days post-transfection or post-infection according to the manufacturers' protocol (Promega). The signal was detected by Vmax ELISA reader (Molecular Devices).

Western blot analysis

COS-7 cells were transfected with Lipofectamine 2000 (Invitrogen) or Fugen6 (Roche, Basel, Switzerland) according to the manufacturer's protocol with proviral DNA encoding the D25N protease mutant. At 48 h post-transfection, cells were washed with PBS and lysed in a buffer containing 4% SDS, 100 mM Tris-HCl (pH 6.8), 12% 2-ME, 20% glycerol and bromophenol blue.

Samples were boiled for 10 min. Protein lysates approximately equivalent to 5×10^4 cells were separated in 5–20% SDS-PAGE (Perfect NT Gel, DRC, Tokyo, Japan), transferred to a polyvinylidene fluoride (PVDF) membrane (Immobilon-P^{SQ}; Millipore, Billerica, MA, USA), and blocked with 5% dried non-fat milk (Yuki-Jirushi, Tokyo, Japan) in PBS. For the primary antibody, we used rabbit anti-*Gag* polyclonal antibody or mouse anti-*Gag* monoclonal antibody. For the secondary antibody, either a biotinylated anti-rabbit antibody or a biotinylated anti-mouse goat antibody (GE Healthcare Bio-Science, Piscataway, NJ, USA) was used. For the tertiary probe, a horseradish peroxidase-conjugated streptoavidin (GE Healthcare Bio-Science) was used. Signals were developed by incubating blots with a chemilumenescent horseradish peroxidase substrate (GE Healthcare Bio-Science) and detected by using Lumi-Imager F1 (Roche).

Results

The structure of sparsomycin, a metabolite from *Streptomyces sparsogenes,* is unique in that it comprises two unusual entities, a monooxodithioacetal moiety and a uracil acrylic acid moiety (Figure 1A). H9 cells were infected with HIV-1 and then maintained in the presence of varying concentrations of sparsomycin. Dimethyl sulphoxide was added in the absence of sparsomycin throughout this study. At 7 days post-infection, a massive syncytial formation was found in the presence of sparsomycin (Figure 1B). The higher the concentration of sparsomycin, the faster p24 accumulated in the culture supernatants (Figure 1C). Similar observations were made in Jurkat, SupT1 (Figures 1D and E), and HPB-Ma cells although the speed of p24 accumulation appeared different among the cell lines. On the other hand, sparsomycin did not show any detectable effect on the cell growth under concentrations of 500 nM.

These results could be due to sparsomycin's ability to either boost HIV-1 replication or select a mutant that replicated substantially faster than the wt HIV-1. To differentiate these possibilities, we recovered the virus-containing culture supernatants from the H9 cell culture at the peak of HIV-1 replication in the presence of 400 nM sparsomycin (asterisk in Figure 1F). Then fresh H9 cells were infected with the recovered virus, the cells were split into two samples and 400 nM of sparsomycin was added to each sample. If sparsomycin selected fast-growing mutants, the replication profiles of HIV-1 should resemble the original sample with sparsomycin (solid circle, Figure 1F) regardless of sparsomycin's presence. However, the replication profile in the presence of sparsomycin shifted leftward (Figure 1G), suggesting that it was unlikely that sparsomycin selected the fast-replicating viral mutants. Therefore, it is likely that sparsomycin boosted HIV-1 replication. Replication-enhancing effects were also seen by using the chemically-synthesized derivatives of sparsomycin (unpublished data; Nakajima *et al.*, 2003). The replication-boosting effect levelled-out at 500 nM, an approximately 20-fold lower concentration than the 50% toxic dose (TD_{50}) of sparsomycin (Ash *et al.*, 1984).

To demonstrate the usefulness of sparsomycin in HIV-1 research, we have examined whether sparsomycin can also boost the replication of drug-resistant low-fitness isolates. The D30N and L90M are common drug-resistant mutations found within HIV-1 protease in HIV-1-infected patients on HAART (Devereux *et al.*, 2001; Kantor *et al.*, 2002; Pellegrin *et al.*, 2002; Sugiura *et al.*, 2002). We introduced proviral DNA carrying the D30N or L90M mutation into H9, Jurkat, and SupT1 cells. HIV-1 replication was than monitored in the presence of 400 nM of sparsomycin. The replication of both viral mutants was substantially enhanced in the presence of sparsomycin in H9 cells (Figures 2A and B). The replication of the L90M-carrying mutant was also enhanced in Jurkat and SupT1 cells (Figures 2C and D). Of note, the replication enhancement appeared profound when HIV-1 displayed relatively slower replication kinetics (for example, the replication of D30N-carrying mutant versus the wt HIV-1 in H9 cells or the replication of HIV-1 in SupT1 versus H9 cells).

Considering the use of sparsomycin in the phenotypic resistance testing, it is critical to know whether sparsomycin affects HIV-1's sensitivity to the antiretroviral drugs. The respective IC_{50} of representative antiretroviral drugs in the absence and the presence of 400 nM sparsomycin were as follows: reverse transcriptase inhibitors; lamivudine, 13.7 and 10.4 nM, and stavudine, 6.3 and 17.0 nM; an non-nucleoside reverse transcriptase inhibitor, nevirapine, 78.2 and 146.4 nM; and protease inhibitors, nelfinavir, 2.8 and 1.0 nM, indinavir, 4.2 and 3.0 nM, and amprenavir, 3.4 and 3.3 nM. Then, we examined whether the presence of sparsomycin affected the IC_{50} of both zidovudine (AZT) and lopinavir (LPV) against a multidrug-resistant HIV-1 isolate, DR3577. The magnitude of both AZT and LPV-resistance of DR3577 was in the order of 2 log (data not shown). The IC_{50}s of AZT in the presence and absence of 400 nM sparsomycin were 14.0 and 36.7 nM, respectively, and for LPV they were 103.1 and 78.9 nM, respectively. These data suggested that the presence of sparsomycin did not significantly influence the IC_{50} of antiretroviral drugs on the replication of both wt and drug-resistant HIV-1.

Finally, we investigated the possible mechanisms that sparsomycin enhanced the replication of HIV-1 and its mutants although the estimated magnitude of enhancement per single replication cycle was small. To do this, we used non-T cells to increase the sensitivity of assays. First, we examined if the early phase of HIV-1's life cycle was

Figure 1. The enhancement of HIV-1 replication by sparsomycin

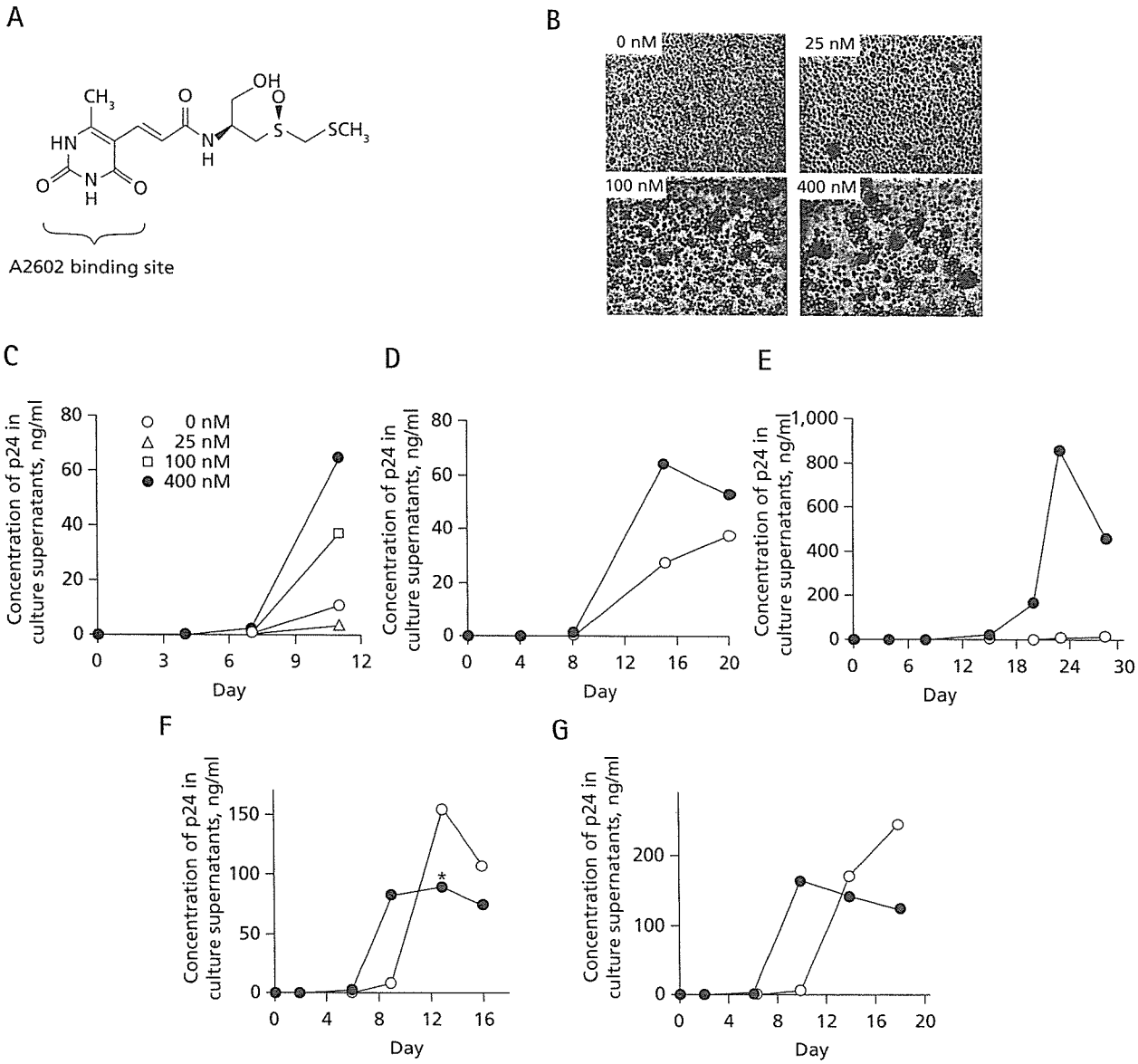

(A) Structure of sparsomycin. The uracil acrylic acid moiety confers the binding capacity to the conserved nucleobase A2602 of the large ribosomal subunit. **(B)** H9 cells infected with HIV-1 were photographed at a week after infection (magnification, ×200). **(C)** The replication profiles of HIV-1 in H9 cells in the presence of varying concentrations of sparsomycin. **(D-G)**. The replication profiles of HIV-1 in Jurkat **(D)**, SupT1 **(E)**, and H9 cells **(F and G)** in the presence of sparsomycin (400 nM, solid circle) or in the absence (open circle; **F and G**). Virus-containing culture supernatant was collected at 13 days post-infection (asterisk, **F**) to infect fresh H9 cells and the replication profiles of HIV-1 were analysed in the presence of sparsomycin (400 nM, solid circle) or in the absence (open circle, **G**).

positively affected by sparsomycin. In the presence of increasing concentrations of sparsomycin, 293 $CD4^+$ T-cells and NP2 CD4 CXCR4 cells were infected with either a replication-deficient HIV-1 vector enveloped with its own *Env* or a VSV-G-psueodotyped MLV vector. Two days post-infection, cells were lysed to measure the luciferase activities representing the efficiency of viral infection. Our results indicate that luciferase activities were not significantly increased at the replication-enhancing dose for both HIV-1 and MLV vectors (Figure 3A). Thus suggesting that the early phase of the retroviral life cycle was not detectably affected by sparsomycin.

Figure 2. Sparsomycin's ability to enhance replication of low-fitness drug resistant HIV-1 mutants

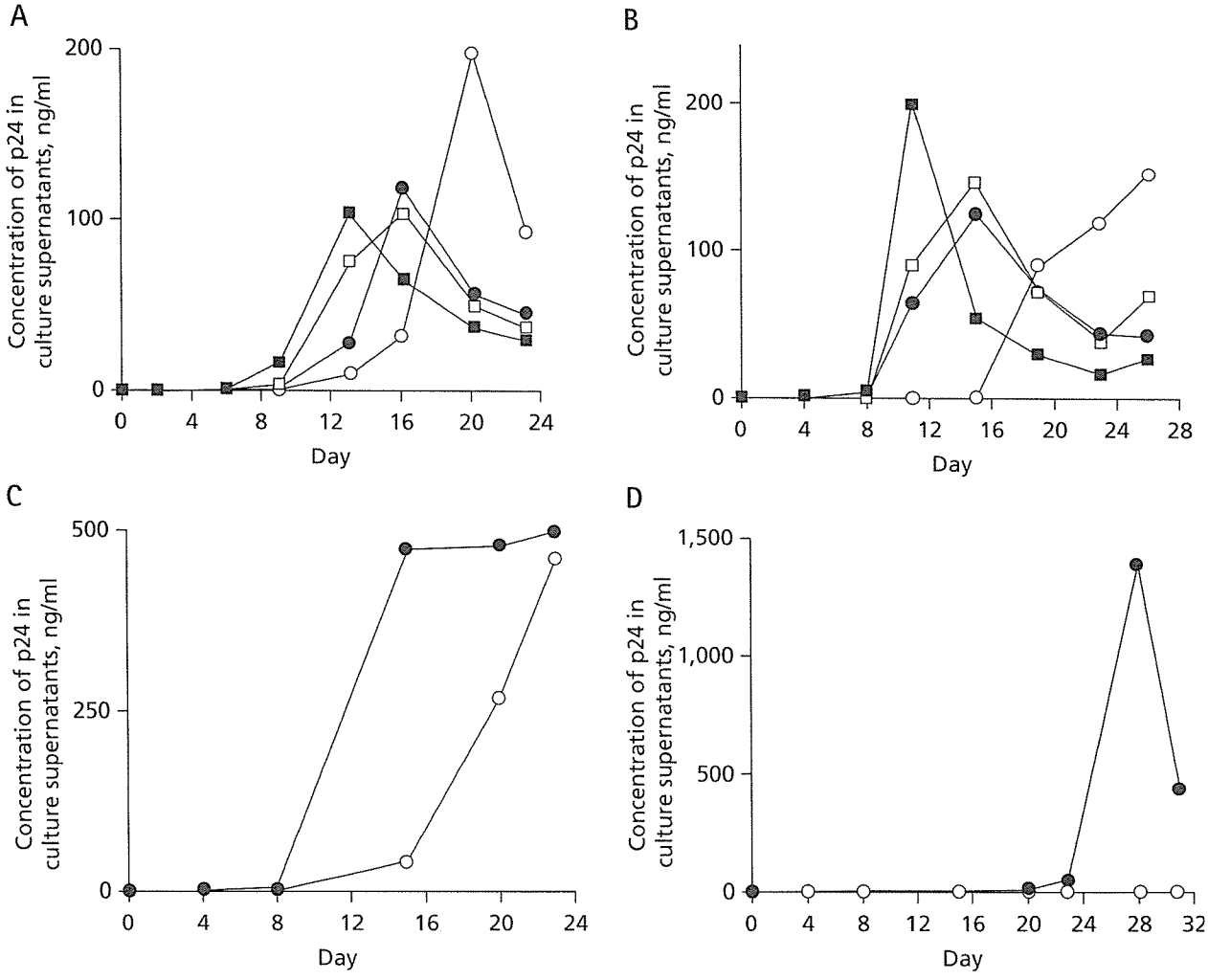

(A and B) The replication kinetics of the D30N-carrying (circle) and L90M-carrying (square) mutants in the presence of sparsomycin (400 nM, solid) or in the absence (open) were investigated twice independently in H9 cells. **(C and D)** The replication kinetics of the L90M-carrying mutant were examined in Jurkat cells **(C)** and SupT1 cells **(D)** in the presence of sparsomycin (400 nM, solid circle) or in the absence (open circle).

Next, we examined the possible active role of sparsomycin in the late phase of HIV-1's life cycle. Sparsomycin has been reported to be a potential enhancer of the −1 frameshift (Dinman *et al.*, 1997). Therefore, we tested whether sparsomycin could positively affect the efficiency of the translational −1 slip at HIV-1's frameshift signal using the reporter assay system established by Dulude *et al.* (2002). The −1 frameshift reporter was created by placing the firefly luciferase in the *pol* frame, pLuc(−1), whereas the control plasmid pLuc(0) has the luciferase in the *gag* frame after the frameshift signal (Figure 3B). In addition, HIV-1's LTR-driven luciferase reporter constructs were tested (pLTR Luc and pLTRΔnefLuc; Figure 3B). We transfected these reporter plasmids into 293T cells along with the renilla luciferase-expressing plasmid phRL/CMV (Promega) to measure the non-specific or toxic effects, if any, of sparsomycin. Cells were incubated in the presence of varying concentrations of sparsomycin for 3 days. Then the dual luciferase assay was performed. The pLuc(−1) behaved differently from the other groups in that the luciferase activities from the pLuc(−1) increased in a dose-dependent fashion. The magnitude of increasement was 2.3-fold at the replication-enhancing dose (Figure 3C). The positive correlation between the relative luciferase activity and the concentration of sparsomycin was statistically significant (r=0.926, P<0.001, n=8, Student's t-test). In contrast, the luciferase activities from the other reporters, even the renilla luciferase plasmid

co-transfected with the pLuc(-1) vector, remained unchanged (Figure 3C). These data suggested that sparsomycin positively affected the efficiency of HIV-1's –1 frameshift. It also suggested that sparsomycin did not enhance transcription from the viral promoter or the translation of proteins driven by the LTR promoter to enhance HIV-1 replication.

If the efficiency of –1 frameshift was increased, we would expect that the *Gag–Pol* to *Gag* ratio to increase. To test this, we transfected COS-7 cells with the HIV-1's proviral DNA carrying the D25N mutation in protease that produced catalytically inactive protease to increase the sensitivity of detecting *Gag–Pol* (Xie *et al.*, 1999). When sparsomycin was added, the intensities of *Gag–Pol* gradually increased in relation to the reporter assay. The *Gag–Pol* to *Gag* ratio reached 1.3-fold at 400 nM sparsomycin when normalized with results produced in the absence of sparsomycin (Figure 3D). The average and standard deviation of the *Gag–Pol* to *Gag* ratio from four independent experiments were 1.29 ± 0.14 at the replication enhancing concentration of sparsomycin (1.29-, 1.48-, 1.16-, and 1.24-fold increase). Similar results were obtained by using

Figure 3. The possible mechanism of HIV-1 replication enhancement by sparsomycin

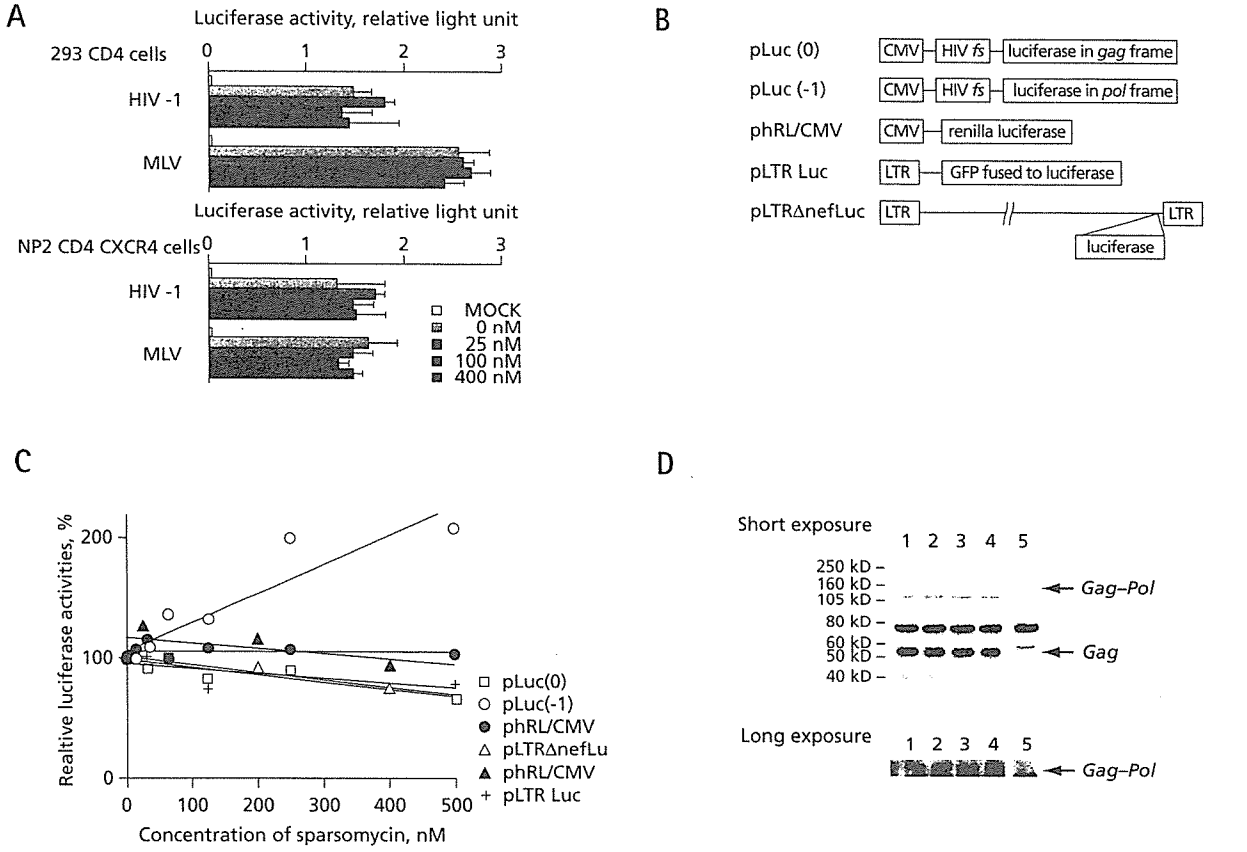

(A) The single round infection efficiencies of HIV-1 and murine lukaemia virus (MLV) vectors measured by the virally-encoded luciferase activities in 293 $CD4^+$ T-cells and NP2 CD4 CXCR4 cells in the presence of varying concentrations of sparsomycin. **(B)** The schematic drawing of constructs used in the reporter assay. The HIV-1's frameshift signal (*fs*) was placed between the CMV promoter and the luciferase. The luciferase was placed in either the *gag* frame (pLuc(0)) or the *pol* frame (pLuc(-1)). The renilla luciferase expression vector phRL/CMV was used in parallel. The pLTR Luc encodes the GFP-luciferase driven by HIV-1's LTR promoter. The pLTRΔnefLuc has the renilla luciferase substituting *nef* in the proviral context of HXB2. **(C)** The luciferase activities from the above reporter constructs without sparsomycin were set as 100% and the relative luciferase activities in the presence of sparsomycin were shown. The renilla luciferase activities from phRL/CMV were shown for the pLuc(-1) (solid circle) and pLTRΔnefLuc (solid triangle) transfections in particular. The pLuc(-1) behaved differently from the other groups and the positive correlation between the relative luciferase activity and the concentration of sparsomycin was statistically significant (r=0.926, P<0.001, n=8, Student's t-test). The SD was within 10% from the avgerage. Shown are the representative data from two independent experiments. **(D)** Western blot analysis to measure the *Gag–Pol* and *Gag* ratio. Cell extracts were separated in the SDS-polyacrylamide gel and immunoblotted by using the rabbit polyclonal antibodies raised against p24. (lane 1, 0 nM; lane 2, 20 nM; lane 3, 200 nM; lane 4, 400 nM; lane 5, MOCK). The lower panel shows the *Gag–Pol* signal obtained from the long exposure of the same blot.

two different antibodies recognizing *Gag*. We were unable to detect a significant increase in the *Env*:*Gag* ratio (unpublished data), suggesting that the sparsomycin's effect on *Gag–Pol*:*Gag* ratio was specific. These data suggested that the translational efficiencies of viral proteins were not equally enhanced by sparsomycin. Altogether, it was strongly suggested that the sparsomycin's replication-boosting effect on HIV-1 was partly due to the enhancement of the –1 frameshift efficiency.

Discussion

In the present study, we have demonstrated that sparsomycin is an enhancer of HIV-1 replication in many human T cell lines at concentrations between 400–500nM. Our preliminary observation suggested that HIV-1 replication was also enhanced in primary peripheral blood monocyte culture (data not shown). Sparsomycin should be able to accelerate the study on the low-fitness HIV-1 such as drug-resistant mutants. As sparsomycin did not alter the IC_{50} of multiple antiretroviral drugs on both wt and drug-resistant HIV-1, its usage should be able to facilitate the phenotypic resistance testing of clinical isolates and as a result, benefit HIV-1-infected patients. Our observation raised an immediate concern as to whether sparsomycin-producing Streptomyces species caused an opportunistic infection in humans, which influenced AIDS progression. However, we did not find any reports suggesting so.

Sparsomycin and puromycin are the only antibiotics that can inhibit protein synthesis in bacterial, archaeal and eukaryotic cells (Ottenheijm *et al.*, 1986; Porse *et al.*, 1999). Sparsomycin has the ability to enhance the –1 frameshift in mammalian cells as well as *S. cervisiae* (Dinman *et al.*, 1997). The proposed molecular mechanism behind this ability was either through a higher affinity of the donor stem for the ribosome and slowing down the rate of the peptidyl transfer reaction, or a change in the steric alignment between donor and acceptor tRNA stems resulting in decreased peptidyl-transfer rates. Conversely, puromycin is not known to enhance the –1 frameshift in mammalian cells. At sub-toxic concentrations, puromycin was unable to enhance the HIV-1 replication (unpublished data). These data, along with the data provided in this paper, implied that the sparsomycin's unique ability to enhance the –1 frameshift might play a role in boosting the HIV-1 replication.

The maintenance of the –1 frameshift efficiency at the optimal range is critical for HIV-1 to replicate (Jacks *et al.*, 1988). Therefore, limiting *Gag–Pol* production should lead to an inhibition of viral replication because *pol* encodes enzymes essential for viral replication (Levin *et al.*, 1993). In contrast, it was also reported that increasing the *Gag–Pol* to *Gag* ratio by twofold resulted in a reduction of viral replication (Hung *et al.*, 1998; Shehu-Xhilaga *et al.*, 2001). Thus, a modest alteration of the –1 frameshift efficiency should markedly affect the replication capacity of HIV-1. Our data indicated that sparsomycin increased the efficiency of –1 frameshift by 1.3-fold, which produces a better replication capacity for HIV-1. As a result, we hypothesize that HIV-1 has a 'suboptimal' –1 frameshift efficiency. In theory, the 1.3-fold difference per one replication cycle becomes approximately 10-fold after 10 rounds of viral replication cycle because the effect accumulates exponentially. The difference should become larger when HIV-1 replicates with the slower kinetics and the replication profile is monitored over a longer time course. In fact, our experimental data were in good agreement with the above estimation. In nature, HIV-1 does not accumulate mutations within the frameshift signal to achieve the higher frameshift efficiencies. This implies that there are multiple and complex regulatory mechanisms that keep the efficiency of the –1 frameshift at suboptimum. Under these conditions, the best efficiency of HIV-1 survival in the host might be achieved. Altogether, one of the possible mechanisms that sparsomycin boosted the HIV-1 replication could be the enhancement of the –1 frameshift efficiency.

Acknowledgements

We thank Drs Hironori Sato and Tsutomu Murakami for critical reading of the manuscript. This work was partly supported by both the Japan Health Science Foundation and the grant from Japanese Ministry of Health, Labor, and Welfare.

References

Ash RJ, Fite LD, Beight DW & Flynn GA (1984) Importance of the hydrophobic sulfoxide substituent on nontoxic analogs of sparsomycin. *Antimicrobial Agents and Chemotherapy* **25**:443–445.

Boden D, Hurley A, Zhang L, Cao Y, Guo Y, Jones E, Tsay J, Ip J, Farthing C, Limoli K, Parkin N & Markowitz M (1999) HIV-1 drug resistance in newly infected individuals. *Journal of the American Medical Association* **282**:1135–1141.

Devereux HL, Emery VC, Johnson MA & Loveday C (2001) Replicative fitness *in vivo* of HIV-1 variants with multiple drug resistance-associated mutations. *Journal of Medical Virology* **65**:218–224.

Dinman JD, Ruiz-Echevarria MJ, Czaplinski K & Peltz SW (1997) Peptidyl-transferase inhibitors have antiviral properties by altering programmed -1 ribosomal frameshifting efficiencies: development of model systems. *Proceedings of the National Academy of Sciences of the United States of America* **94**:6606–6611.

Dulude D, Baril M & Brakier-Gingras L (2002) Characterization of the frameshift stimulatory signal controlling a programmed -1 ribosomal frameshift in the human immunodeficiency virus type 1. *Nucleic Acids Research* **30**:5094–5102.

Gehringer H, Bogner JR, Goebel FD, Nitschko H & von der Helm K (2000) Sequence analysis of the HIV-1 protease coding region of 18 HIV-1-infected patients prior to HAART and possible implications on HAART. *Journal of Clinical Virology* **17**:137–141.

Hertogs K, de Bethune MP, Miller V, Ivens T, Schel P, Van Cauwenberge A, Van Den Eynde C, Van Gerwen V, Azijn H, Van Houtte M, Peeters F, Staszewski S, Conant M, Bloor S, Kemp S, Larder B & Pauwels R (1998) A rapid method for simultaneous detection of phenotypic resistance to inhibitors of protease and reverse transcriptase in recombinant human immunodeficiency virus type 1 isolates from patients treated with antiretroviral drugs. *Antimicrobial Agents and Chemotherapy* **42:**269–276.

Hirsch, MS, Brun-Vezinet F, D'Aquila RT, Hammer SM, Johnson, VA, Kuritzkes DR, Loveday C, Mellors JW, Clotet B, Conway B, Demeter LM, Vella S, Jacobsen DM & Richman DD (2000) Antiretroviral drug resistance testing in adult HIV-1 infection: recommendations of an International AIDS Society-USA Panel. *Journal of the American Medical Association* **283:**2417–2426.

Hung M, Patel P, Davis S & Green SR (1998) Importance of ribosomal frameshifting for human immunodeficiency virus type 1 particle assembly and replication. *Journal of Virology* **72:**4819-4824.

Iga M, Matsuda Z, Okayama A, Sugiura W, Hashida S, Morishita K, Nagai Y & Tsubouchi H (2002) Rapid phenotypic assay for human immunodeficiency virus type 1 protease using *in vitro* translation. *Journal of Virological Methods* **106:**25–37.

Jacks T, Power MD, Masiarz FR, Luciw PA, Barr PJ & Varmus HE. (1988) Characterization of ribosomal frameshifting in HIV-1 gag-pol expression. *Nature* **331:**280–283.

Jarmy G, Heinkelein M, Weissbrich B, Jassoy C & Rethwilm A (2001) Phenotypic analysis of the sensitivity of HIV-1 to inhibitors of the reverse transcriptase, protease, and integrase using a self-inactivating virus vector system. *Journal of Medical Virology* **64:**223–231.

Kantor R, Fessel WJ, Zolopa AR, Israelski D, Shulman N, Montoya JG, Harbour M, Schapiro JM & Shafer RW (2002) Evolution of primary protease inhibitor resistance mutations during protease inhibitor salvage therapy. *Antimicrobial Agents and Chemotherapy* **46:**1086–1092.

Kellam P & Larder BA (1994) Recombinant virus assay: a rapid, phenotypic assay for assessment of drug susceptibility of human immunodeficiency virus type 1 isolates. *Antimicrobial Agents and Chemotherapy* **38:**23–30.

Komano J, Miyauchi K, Matsuda Z & Yamamoto N (2004). Inhibiting the Arp2/3 Complex limits infection of both intracellular mature vaccinia virus and primate lentiviruses. *Mol Biol Cell* **15:**5197–5207.

Levin JG, Hatfield DL, Oroszlan S & Rein A (1993) Mechanisms of translational suppression used in the biosynthesis of reverse transcriptase. In *Reverse transcriptase*, pp. 5–31. Edited by AM Skalka & SP Goff. New York: Cold Spring Harbor Laboratory Press.

Matsuda Z, Yu X, Yu QC, Lee TH & Essex M (1993) A virion-specific inhibitory molecule with therapeutic potential for human immunodeficiency virus type 1. *Proceedings of the National Academy of Sciences of the United States of America* **90:**3544–3548.

Menzo S, Rusconi S, Monachetti A, Colombo MC, Violin M, Bagnarelli P, Varaldo PE, Moroni M, Galli M, Balotta C & Clementi M (2000) Quantitative evaluation of the recombinant HIV-1 phenotype to protease inhibitors by a single-step strategy. *AIDS* **14:**1101–1110.

Miyauchi K, Komano J, Yokomaku Y, Sugiura W, Yamamoto N & Matsuda, Z (2005) Role of the specific amino acid sequence of the membrane-spanning domain of human immunodeficiency virus type 1 in membrane fusion. *Journal of Virology* **79:**4720–4729.

Nakajima N, Enomoto T, Watanabe T, Matsuura N & Ubukata M. (2003) Synthesis and activity of pyrimidinylpropenamide antibiotics: the alkyl analogues of sparsomycin. *Bioscience, Biotechnology, and Biochemistry* **67:**2556–2566.

Ottenheijm HC, van den Broek LA, Ballesta JP & Zylicz Z (1986) Chemical and biological aspects of sparsomycin, an antibiotic from Streptomyces. *Progress in Medicinal Chemistry* **23:**219–268.

Parkin NT, Chappey C & Petropoulos CJ (2003) Improving lopinavir genotype algorithm through phenotype correlations: novel mutation patterns and amprenavir cross-resistance. *AIDS* **17:**955–961.

Pellegrin I, Breilh D, Montestruc F, Caumont A, Garrigue I, Morlat P, Le Camus C, Saux MC, Fleury HJ & Pellegrin JL (2002) Virologic response to nelfinavir-based regimens: pharmacokinetics and drug resistance mutations (VIRAPHAR study). *AIDS* **16:**1331–1340.

Porse BT, Kirillov SV, Awayez MJ, Ottenheijm HC & Garrett RA (1999) Direct crosslinking of the antitumor antibiotic sparsomycin, and its derivatives, to A2602 in the peptidyl transferase center of 23S-like rRNA within ribosome-tRNA complexes. *Proceedings of the National Academy of Sciences of the United States of America* **96:**9003–9008.

Rodriguez-Rosado R, Briones C & Soriano V (1999) Introduction of HIV drug-resistance testing in clinical practice. *AIDS* **13:**1007–1014.

Sarmati L, Nicastri E, Parisi SG, d'Ettorre G, Mancino G, Narciso P, Vullo V & Andreoni M (2002) Discordance between genotypic and phenotypic drug resistance profiles in human immunodeficiency virus type 1 strains isolated from peripheral blood mononuclear cells. *Journal of Clinical Microbiology* **40:**335–340.

Shehu-Xhilaga M, Crowe SM & Mak J (2001) Maintenance of the Gag/Gag-Pol ratio is important for human immunodeficiency virus type 1 RNA dimerization and viral infectivity. *Journal of Virology* **75:**1834–1841.

Sugiura W, Matsuda Z, Yokomaku Y, Hertogs K, Larder B, Oishi T, Okano A, Shiino T, Tatsumi M, Matsuda M, Abumi H, Takata N, Shirahata S, Yamada K, Yoshikura H & Nagai Y (2002) Interference between D30N and L90M in selection and development of protease inhibitor-resistant human immunodeficiency virus type 1. *Antimicrobial Agents and Chemotherapy* **46:**708–715.

Walter H, Schmidt B, Korn K, Vandamme AM, Harrer T & Uberla K. (1999). Rapid, phenotypic HIV-1 drug sensitivity assay for protease and reverse transcriptase inhibitors. *Journal of Clinical Virology* **13:**71–80.

Xie D, Gulnik S, Gustchina E, Yu B, Shao W, Qoronfleh W, Nathan A & Erickson JW (1999) Drug resistance mutations can effect dimer stability of HIV-1 protease at neutral pH. *Protein Science* **8:**1702–1707.

Yerly S, Kaiser L, Race E, Bru JP, Clavel F & Perrin L (1999) Transmission of antiretroviral-drug-resistant HIV-1 variants. *Lancet* **354:**729–733.

Received 5 December 2005, accepted 23 March 2006

Molecular Biology of the Cell
Vol. 15, 5197–5207, December 2004

Inhibiting the Arp2/3 Complex Limits Infection of Both Intracellular Mature Vaccinia Virus and Primate Lentiviruses

Jun Komano,* Kosuke Miyauchi, Zene Matsuda, and Naoki Yamamoto

Laboratory of Virology and Pathogenesis, AIDS Research Center, National Institute of Infectious Diseases, Tokyo 208-0011, Japan

Submitted April 2, 2004; Revised September 6, 2004; Accepted September 13, 2004
Monitoring Editor: Thomas Pollard

Characterizing cellular factors involved in the life cycle of human immunodeficiency virus type 1 (HIV-1) is an initial step toward controlling replication of HIV-1. Actin polymerization mediated by the Arp2/3 complex has been found to play a critical role in some pathogens' intracellular motility. We have asked whether this complex also contributes to the viral life cycles including that of HIV-1. We have used both the acidic domains from actin-related protein (Arp) 2/3 complex-binding proteins such as the Wiscott-Aldrich syndrome protein (N-WASP) or cortactin, and siRNA directing toward Arp2 to inhibit viral infection. HIV-1, simian immunodeficiency virus (SIV), and intracellular mature vaccinia virus (IMV) were sensitive to inhibition of the Arp2/3 complex, whereas MLV, HSV-1, and adenovirus were not. Interestingly, pseudotyping HIV-1 with vesicular stomatitis virus G protein (VSV-G) overcame this inhibition. Constitutive inhibition of the Arp2/3 complex in the T-cell line H9 also blocked replication of HIV-1. These data suggested the existence of an Arp2/3 complex-dependent event during the early phase of the life cycles of both primate lentiviruses and IMV. Inhibiting the HIV-1's ability to activate Arp2/3 complex could be a potential chemotherapeutic intervention for acquired immunodeficiency syndrome (AIDS).

INTRODUCTION

When human immunodeficiency virus type 1 (HIV-1) enters cells, the envelope glycoprotein gp120 binds to CD4 and subsequently CXCR4 or CCR5 and initiates membrane fusion at the cell surface. After the membrane fusion the reverse transcription takes place while the viral core components migrate toward cell nucleus where the proviral DNA integrates into the host cell chromosome. However, the protein-protein interactions during these processes of disassembly/uncoating are the least understood among the whole viral life cycle. Despite historical suggestions that actin plays a role in the early phase of HIV-1 infection, its role remains largely unclear. Early studies used chemical inhibitors of actin, which were broadly active on cell physiology or "nonspecific" (Cudmore *et al.*, 1997; Bukrinskaya *et al.*, 1998; Iyengar *et al.*, 1998). To test for a specific role of actin in the early phase of HIV-1's life cycle, we focused on regulators of actin polymerization. It has now been shown that some bacteria and viruses use cellular actin polymerization to propel themselves within cells (Gruenheid and Finlay, 2003). The key host proteins in these reactions are actin-related protein (Arp) 2/3 complex and its regulators. We hypothesized that Arp2/3 complex-dependent actin nucleation might be required for efficient infection by primate lentiviruses including HIV-1.

The Arp2/3 complex is a seven-subunit protein complex highly conserved among eukaryotes that nucleates actin filaments from the sides of existing filaments (Higgs and Pollard, 2001; Pantaloni *et al.*, 2001). The Arp2/3 complex distributes throughout the cell but is enriched especially at the cortical layer underneath the plasma membrane through which viruses have to pass to infect cells (Flanagan *et al.*, 2001). The Arp2/3 complex is regulated by both Wiscott-Aldrich syndrome protein (WASP) family of proteins and cortactin (Weaver *et al.*, 2003). The carboxy terminal domain of WASP is called VCA domain (verprolin homology, cofilin homology and acidic subdomains) and is also named the WA domain. Intensive studies had revealed that VCA's ability to bind monomer actin through its V subdomain is critical for actin nucleation (Miki and Takenawa, 1998). The CA subdomain confers to N-WASP its binding ability to the Arp2/3 complex as evidenced by physicochemical assays (Machesky and Insall, 1998; Marchand *et al.*, 2001) and x-ray crystallography and cross-linking experiments (Gournier *et al.*, 2001; Robinson *et al.*, 2001; Zalevsky *et al.*, 2001). Actin polymerization, nucleation, and branching are enhanced in the presence of VCA protein in vitro (Higgs *et al.*, 1999; Machesky *et al.*, 1999; Rohatgi *et al.*, 1999). Expression of the VCA protein sequesters the Arp2/3 complex and displaces it from physiological regulation in vivo (Machesky and Insall, 1998; Machesky *et al.*, 1999; Rozelle *et al.*, 2000; Castellano *et al.*, 2001; Harlander *et al.*, 2003). By expressing in tissue culture cells, the VCA protein has been used successfully as an inhibitor of Arp2/3 complex to study the role of

Article published online ahead of print. Mol. Biol. Cell 10.1091/mbc.E04-04-0279. Article and publication date are available at www.molbiolcell.org/cgi/doi/10.1091/mbc.E04-04-0279.

* Corresponding author. E-mail address: ajkomano@nih.go.jp.

Abbreviations used: Arp2/3, actin-related protein 2/3; CC, cytochalasin; GFP, green fluorescent protein; HIV-1, human immunodeficiency virus type 1; HSV-1, herpes simplex virus type 1; IMV, intracellular mature virus; MLV, murine leukemia virus; RLU, relative light unit; SIV, simian immunodeficiency virus; VSV-G, vesicular stomatitis virus G protein; VV, vaccinia virus; WASP, Wiscott-Aldrich syndrome protein.

Arp2/3 complex in many biologic processes (Zhang *et al.*, 1999; Krause *et al.*, 2000; May *et al.*, 2000; Moreau *et al.*, 2000; Rozelle *et al.*, 2000; McGee *et al.*, 2001; Zhang *et al.*, 2002).

Another Arp2/3 complex regulator is cortactin, a filamentous actin-associated protein originally identified as a substrate of *Src* (Weed and Parsons, 2001) that is also implicated in the phagocytosis of several invasive bacteria (Dehio *et al.*, 1995; Fawaz *et al.*, 1997; Cantarelli *et al.*, 2000). Cortactin binds directly to the Arp2/3 complex through its amino-terminal acidic domain, NTA, and activates it (Weed *et al.*, 2000; Uruno *et al.*, 2001; Weaver *et al.*, 2001). The NTA protein, like VCA, can serve as an inhibitor of Arp2/3 complex.

We explored the possible involvement of Arp2/3 complex in the early phase of life cycle of primate lentiviruses. In parallel, we tested different virus species including adenovirus, herpes simplex virus type 1 (HSV-1), Moloney murine leukemia virus (MLV), and intracellular mature vaccinia virus (IMV), all of which were reported to use the actin cytoskeleton to infect cells; however, the physical properties and mechanisms of their entry vary (Rosenthal *et al.*, 1985; Kizhatil and Albritton, 1997; Bukrinskaya *et al.*, 1998; Iyengar *et al.*, 1998; Li *et al.*, 1998). We also tested whether changing retroviral envelopes, which forces viruses to enter through different routes, affected the efficiencies of viral entry.

MATERIALS AND METHODS

Cells and Viruses

Human embryonic kidney (HEK) 293 cells and Chinese hamster ovary (CHO)-K1 cells were maintained in Dulbecco's modified Eagle's medium (DMEM, Sigma, St. Louis, MO) supplemented with 10% FBS (Hyclone, Logan, UT), penicillin, and streptomycin (Invitrogen, Carlsbad, CA). H9 cells were maintained in RPMI1640 (Sigma) supplemented with 10% FBS, penicillin, and streptomycin. All the mammalian cell lines were incubated at 37°C in the humidified 5% CO_2 atmosphere. Replication incompetent HIV-1 (HXB2 *vpr, rev, env, nef*) was produced by transfecting the proviral DNA carrying renilla luciferase in place of *nef* open reading frame into 293 T-cells along with the expression plasmid for *env, tat, rev* and *nef* (pIIIex). When pseudotyping HIV-1, *rev* expressing plasmid and either ecotropic MLV envelope (Ragheb and Anderson, 1994) or vesicular stomatitis virus G (VSV-G) expressing plasmid (Clontech, Palo Alto, CA) were cotransfected with the proviral DNA of HIV-1. HXB2 was used for the replication competent HIV-1. The virus was prepared by transfecting the proviral DNA into 293 T-cells, and the supernatants were collected at 2 d posttransfection. SIV (*nef*) encoding firefly luciferase in place of *nef* open reading frame was created based on the IL-2–carrying molecular clone of SIVmac239 (Gundlach *et al.*, 1997; kindly provided by Dr. K. Mori). SIV was prepared by transfecting the proviral DNA into COS7 cells, and the supernatants were collected. MLV was produced by transfecting pCMMP LacZIRESGFP, pCMMP eGFP (generous gift from Dr. J. Young), pCMMP GFP-VCA, or pQcLIN (Clontech) into 293 cells along with *gag/pol* and either ecotropic, amphotropic *env*, or VSV-G–expressing plasmids (Ragheb and Anderson, 1994). HSV-1 (KOS)Rid1/tk12 encoding beta-galactosidase under the regulation of the immediate early promoter ICP4, vaccinia virus encoding T7 RNA polymerase (vTF7.3), and adenovirus type 5 expressing T7 RNA polymerase were generous gifts from Drs. Spear (Dean *et al.*, 1994), Moss (Fuerst *et al.*, 1986), and Ishii (Aoki *et al.*, 1998), respectively, and were prepared according to the previous publications. Adenovirus, HSV-1 and IMV were titrated by the plaque assay using HEK293 or Hela cells; MLV by counting reporter-positive HEK293 cells after 2 to 3 d postinfection, and HIV-1, VSV-G HIV-1, and SIV by using the indicator cells that expressed beta-galactosidase or GFP upon infection. The p24 concentration of eco HIV-1 was adjusted to that of HIV-1 (100 ng/ml). The neutralization assay using the antibody 2D5 that inhibits infection of IMV but not that of EEV (Ichihashi and Oie, 1996) revealed that 99.4% of our vaccinia virus preparation contained intracellular mature virus (IMV).

Plasmids

The VCA domain (amino acid 392–505) of N-WASP was amplified by PCR from N-WASP cDNA kindly provided by Dr. Takenawa (Miki *et al.*, 1996) with the following primers: VCA sense 5 -CAATTGCCTTCTGATGGGGACCATCAGG-3 and 5 -AAGCTTCAGTCTTCCCACTCATCATC-3 . The PCR product was subcloned into pCR4 Blunt TOPO (Invitrogen), sequenced, digested with *Mfe*I and *Eco*RI, and cloned into *Eco*RI site of pEGFP-C2 (Clontech), generating pGFP-VCA. Following two primers, 5 -AGATCTTAGTGGCTGATGGCCAAGAGTC-CACACC-3 and 5 - CAATTGTCAGTCTTCCCACTCATCATC-3 , were used to amplify the CA domain (amino acid 470–505) of N-WASP. The PCR fragment was cloned into *Bgl*II-*Eco*RI sites of pEGFP-C2, giving rise to pGFP-CA. GFP-A expression plasmid was generated by annealing following two oligonucleotides and cloned it into the *Bgl*II-*Eco*RI sites of pEGFP-C2: 5 -GATCGATGAAGATGAAGATGAA-GATGATGAAGAAGATTTTGAGGATGATGATGAGTGGGAAGACTGA-3 and 5 -AATTTCAGTCTTCCCACTCATCATCATCCTCAAAATCTTCTTCATCATCT-TCATCTTCATCTTCATC-3 . Following oligonucleotides were annealed and ligated into the *Bgl*II site of pGFP-VCA giving rise to pGFP-VCA*: 5 -GATCTAGATAACT-GATGCGGCCGCCG-3 and 5 -GATCCGGCGGCCGCATCAGTTATCTA-3 . The NTA domain (amino acid 1–84) of cortactin and Arp2 were amplified by PCR from 293T cDNA with following primers: NTA sense 5 -GGATCCTCGAGATGTG-GAAAGCTTCAGCAGGCCAC-3 , NTA antisense 5 -CAATTGTCAATAGCCAT-GGGAAGCTTTTGGTCC-3 ; Arp2 sense 5 -GGATCCTCGAGATGGACAGC-CAGGGCAGGAAGG-3 , Arp2 antisense 5 -CAATTGTTATCGAACAGTCACAC-CAAGTTTC-3 . PCR fragments were cloned into pCR4 Blunt TOPO, and the *Bam*HI-*Mfe*I fragments were cloned into *Bgl*II-*Eco*RI sites of pEGFP-C2, generating pGFP-NTA and pGFP-Arp2. pCMMP GFP-VCA was generated by digesting pC-MMP GFP with *Age* I and *Bam*HI, ligated with *Age* I-*Bam*HI fragment from pGFP-VCA. Transfection efficiencies were measured by phRL/CMV (Promega, Madison, WI) or pHIV-1 LTR-GFP-Luciferase. F10, the ecotropic MLV receptor from rat, expression plasmid was created by digesting pcDNA F10-ecoR (Takase-Yoden and Watanabe, 1999) with *Nae*I followed by the self-ligation. The human nectin 1 alpha (HigR) expression plasmid was generated by inserting *Eco*RI fragment of pEF-BOS human nectin 1 alpha 3xFLAG (Sakisaka *et al.*, 2001) into *Eco*RI site of pcDNA3 (Invitrogen). The *Xho*I-*Not*I fragment of either pBCMGSneoCD4 or pBCMGS-neoCCR5 (a generous gift from Dr. Yamashita) was cloned into *Xho*I-*Not*I sites of pcDNA3 (Invitrogen), generating pCD4 and pCCR5, respectively. The *Sna*BI-*Not*I fragment from pCCR5 was cloned into pMACS4ires (Miltenyi Biotec, Bergisch Gladbach, Germany), generating pCCR5 IRES CD4. The CD4 lacking the cytoplasmic tail was amplified by the following primers: 5 -GGATCCCGGGCCACCATGA-ACCGGGGAGTCCCTTTTAGGC-3 and 5 - GAATTCGTGCCGGCACCTGACA-CAGAAGAAGATGCC-3 . The *Xma*I-*Eco*RI fragment was cloned into the *Age*I-*Eco*RI sites of pEGFP-C2, generating pCD4 cyt. The T7 RNA polymerase (T7 RNAP) expression plasmid pCMMP T7RNAP IRES GFP was created by inserting *Xma*I-*Eco*RI fragment from pVR1-T7 into *Age*I-*Mfe*I sites of pCMMP IRES GFP (Aoki *et al.*, 1998). The T7RNAP reporter plasmid pTM3Luci was described previously (Aoki *et al.*, 1998). The following pairs of oligonucleotides were annealed and cloned into *Apa*I-*Eco*RI sites of pSilencer 1.0-U6 (Ambion, Austin, TX) to generate siRNA expressing vectors directing against GFP and Arp2: GFP sense 5 -GCTGACCCTGAAGTTC-ATCTTCAAGAGAGATGAACTTCAGGGTCAGCTTTTTT-3 and GFP antisense 5 -AATTAAAAAAGCTGACCCTGAAGTTCATCTCTCTTGAAGATGAACTTC-AGGGTCAGCGGCC-3 ; Arp2 sense 5 -CAGCTTTACTTAGAACGAGTTCAA-GAGACTCGTTCTAAGTAAAGCTGTTTTTT-3 and Arp2 antisense 5 -AATT-AAAAAACAGCTTTACTTAGAACGAGTCTCTTGAACTCGTTCTAAGTAAA-GCTGGGCC-3 .

Transfection, Magnetic Selection, and Infection

Plasmid DNAs were transfected into cells by using either lipofectamin/lipofectamin plus reagent (Invitrogen) or X-tremeGENE siRNA transfection reagent (Roche Diagnostics, Mannheim, Germany) according to the manufacturer's protocol. The latter reagent, with which the transfection efficiencies reached 90% in 293 cells, was specifically used for preparing samples to carry out Western blot analysis demonstrating the reduction of Arp2 levels. In brief, cells were fed in 48-well plates 1–2 d before transfection. Cells were approximately in 50–60% confluency at transfection. After transfection, cells were trypsinized and plated onto 96-well plates. Transfected cells were magnetically selected by using MACS system directing toward CD4 (Miltenyi Biotec). Cells were infected with viruses of 0.1–0.5 multiplicity of infection by incubating in the virus-containing culture medium at 37°C for 1–4 h.

Cell-to-cell Fusion Assay

The fusion assay was based on the T7RNAP transcription-dependent reporter assay originally described by Nussbaum *et al.* (1994), modified versions by Sakamoto *et al.* (2003). In brief, the T7RNAP "donor" cells were generated by transfecting 293 cells with both T7RNAP and HIV-1's Env expression vectors. The T7RNAP "acceptor" cells were generated by transfecting 293 cells with the T7RNAP reporter (pT7-IRES-Luciferase) along with either CD4 or CD4 cyt, GFP or GFP-VCA, and the renilla luciferase expression vectors. At 48 h posttransfection, these cells were cocultivated for 24 h and lysed in the passive lysis buffer to carry out the dual luciferase assay (Promega).

Detection of Fluorescent Signals

The transfected 293 cells were fixed by 4% formaldehyde in PBS at 48 h posttransfection and imaged by using confocal microscopy META 510 (Carl Zeiss, Jene, Germany). For the images showing pseudopodial extensions, images of different focal planes were projected to generate a single image. The transfected H9 cells were imaged similarly at 48 h posttransfection without fixation. The light transmission image was merged with the green fluorescent signal. Alternatively, the transfected cells were analyzed by the flow cytometry (FACS calibur, Becton Dickinson, San Jose, CA).

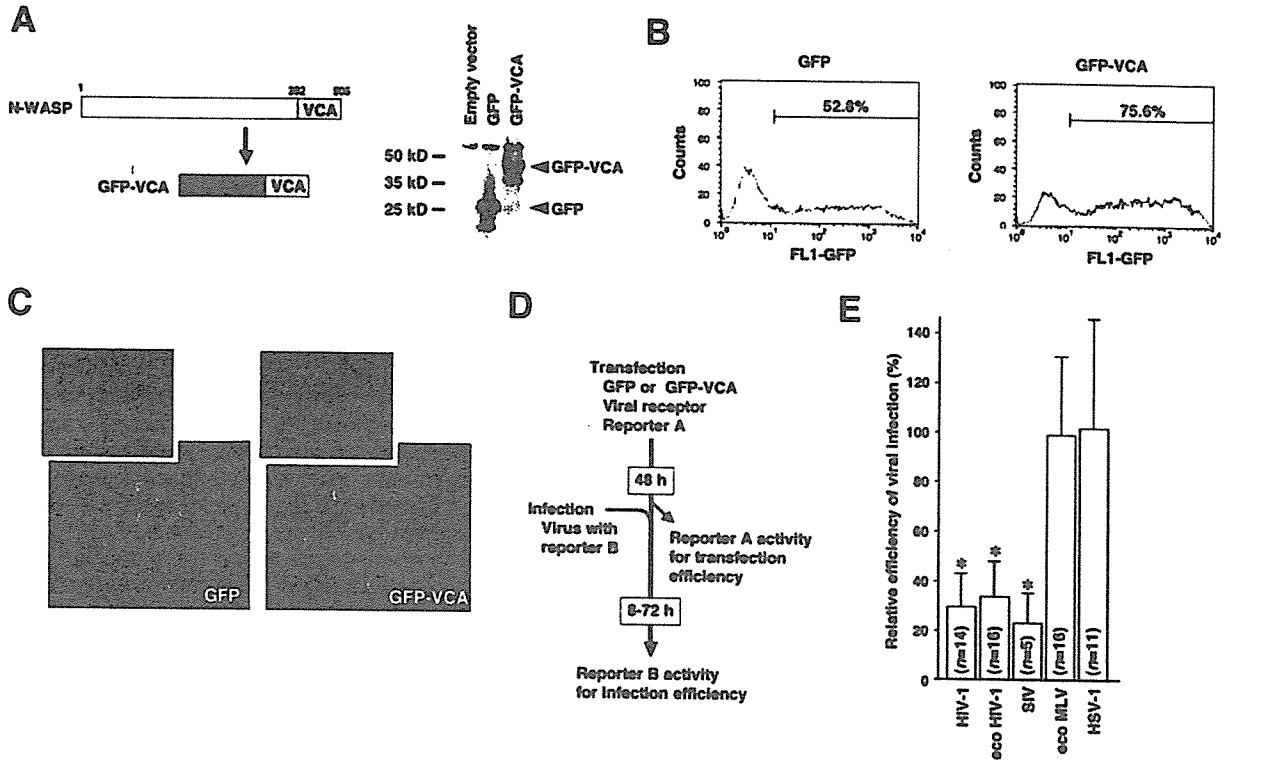

Figure 1. Inhibiting the Arp2/3 complex limited the entry of primate lentiviruses. (A) The carboxy-terminus of N-WASP, VCA domain, was fused to GFP to give rise GFP-VCA. Western blot analysis detected the 41-kDa band, the predicted mol wt for GFP-VCA. (B) The green fluorescence profiles of 293 cells transfected with either GFP or GFP-VCA expression vector were similar to each other as measured by the flow cytometric analysis. (C) GFP-VCA preferentially distributed evenly throughout the cytoplasm. The pseudopodial extension was less active when GFP-VCA was expressed in 293 cells compared with GFP (magnification, 200; inset, 400). (D) The experimental procedure was drawn schematically. (E) The relative infection efficiencies of HIV-1, HIV-1 pseudotyped with ecotropic MLV envelope (eco HIV-1), and SIV into cells expressing GFP-VCA were significantly decreased, whereas those of ecotropic MLV (eco MLV) and HSV-1 were not (asterisk, p 0.01). The data represent the average and SD of indicated number of independent experiments.

Western Blot Analysis

Cells were washed with PBS and lysed in a buffer containing 4% SDS, 100 mM Tris-HCl (pH 6.8), 12% 2-ME, 20% glycerol, and bromophenol blue. Samples were boiled for 10 min. Protein lysates approximately equivalent to 5 10^4 cells were separated in SDS-PAGE (Perfect NT Gel, DRC, Tokyo, Japan), transferred to a polyvinylidene fluoride (PVDF) membrane (Immobilon-P^{SQ}, Millipore, Bedford, MA), and blocked with 5% dried nonfat milk (Yuki-Jirushi, Tokyo, Japan) in PBS. For the primary antibody, we used anti-Arp2 antibody H-84 (Santa Cruz Biotechnology, Santa Cruz, CA), antiactin antibody MAB1501 (Chemicon, Temecula, CA), or either an mAb or a polyclonal rabbit antiserum against GFP (Clontech). For the secondary antibody, either a biotinylated anti-mouse antibody (Amersham Pharmacia Biotech, Piscataway, NJ) or a biotinylated anti-rabbit antibody was used. For the tertiary probe, a horseradish peroxidase (HRP)-conjugated streptoavidin (Amersham Pharmacia Biotech) was used. Signals were developed by incubating blots with the chemilumenescent HRP substrate (Amersham Pharmacia Biotech) and detected by using Lumi-Imager F1 (Boehringer Mannheim, Mannheim, Germany).

Reporter Assays

Cells were lysed in the Passive Lysis Buffer (Promega) and the dual luciferase assay was performed to measure both firefly and renilla luciferase activities according to the manufacturer's protocol (Promega). The beta-galactosidase activity was measured by using the LumiGal assay kit according to the manufacturer's protocol (Clontech). The chemiluminescence was detected by Lmax (Nihon Molecular Devices, Tokyo, Japan).

ELISA

The amount of p24 antigen of HIV-1 in the culture supernatants was quantified by using Retro TEK p24 antigen ELISA kit according to the manufacturer's protocol (Zepto Metrix, Buffalo, NY). The signals were measured by Vmax ELISA reader (Nihon Molecular Devices).

Statistical Analysis

The significance of differences was tested by one-way analysis of variance (ANOVA) and Student's t test. P values 0.05 were considered to be significant.

RESULTS

GFP-VCA Inhibits Infection of Primate Lentiviruses

We first tested whether the viral infection was affected by expressing a potential inhibitor of the Arp2/3 complex GFP-VCA, the VCA domain of N-WASP fused to GFP (Figure 1A). The expression of GFP-VCA protein was verified by Western blot analysis (Figure 1A). The expression levels of GFP-VCA were similar to those of GFP as measured by the flow cytometric analysis at 48 h posttransfection (Figure 1B). GFP-VCA preferentially distributed to the cytoplasm and inhibited the pseudopodial extension compared with GFP alone in agreement with the previous report (Rozelle *et al.*, 2000; Figure 1C). To exclude the possibility that GFP fusion proteins negatively affects the cell surface expression of membrane proteins, we confirmed that the distribution and the levels of transiently and constitutively expressed CD4 and CXCR4 on the cell surface were similar in both GFP- and GFP-VCA–expressing cells as assessed by both confocal microscopy and the flow cytometric analysis (unpublished data).

To evaluate the contribution of the Arp2/3 complex on the viral infection, we used a transient transfection/infection

Table 1. Viruses tested in the receptor-dependent infection system

Virus	Virally encoded reporter	Reporter to normalize infection efficiency	Replication-competency	Infected cells harvested (h postinfection)	Receptor used in this study	S/N ratio[a]
HIV-1	Renilla luciferase	Firefly luciferase	Incompetent	48–72	CD4	4.5
eco HIV-1	Renilla luciferase	Firefly luciferase	Incompetent	48–72	F10	41.2
SIV	Firefly luciferase	Renilla luciferase	Competent	48	CD4 and CCR5	26.4
eco MLV	-galactosidase	Firefly luciferase	Incompetent	48–72	F10	20.8
HSV-1	-galactosidase	Firefly luciferase	Competent	8	HigR	207.4

See Figure 1.

[a] The signal-to-noise ratio was calculated by dividing the virally encoded reporter gene activities in the GFP-expressing cells by the background signal. Data from all the trials shown in Figures 1 and 4 were averaged.

system in which target cells were transfected with a mixture of plasmid DNA expressing 1) an Arp2/3 complex inhibitor GFP-VCA, 2) a viral receptor, and 3) a reporter gene to normalize transfection efficiencies (depicted in Figure 1D). Because of the nature of cotransfection, the majority of cells uptook the expression vector for GFP-VCA were transfected with the other plasmids because the mixture of DNA contained fivefold excess amount of the GFP-VCA expressing plasmid. At 48 h posttransfection, a portion of transfected cells were collected to measure the transfection efficiencies and others were challenged by a virus expressing a reporter gene to monitor the efficiency of infection. Various times after infection, cells were lysed and the virally encoded reporter gene activities were measured, which was divided by the transfection efficiencies to normalize. Infection of viruses was restricted to the transfected cells by using viral receptors: human CD4 for HIV-1, human CD4 and CCR5 for SIV, F10 for ecotropic MLV envelope-pseudotyped HIV-1 (eco HIV-1) and ecotropic MLV (eco MLV), human nectin-1 alpha (HigR) for HSV-1. Viruses, receptors, and the combination of reporter genes for each virus were summarized in Table 1. Primarily we targeted HEK293 cells because actin cytoskeletal system is shared among eukaryotes. To monitor HSV-1 infection, CHO-K1 cells were used that lack entry molecules for HSV-1. To monitor the efficiencies of single-round viral infection, we used replication-incompetent HIV-1 and MLV. Alternatively, cells infected with replication-competent viruses were lysed at time points before viruses entered the second replication cycle, except SIV, which required 48 h to give sufficient signal to be detected. Importantly, all the viruses tested in this study were reported to utilize actin cytoskeleton to infect cells as examined by using chemical inhibitors against actin such as cytochalasin (CC; Rosenthal *et al.*, 1985; Kizhatil and Albritton, 1997; Bukrinskaya *et al.*, 1998; Iyengar *et al.*, 1998; Li *et al.*, 1998). The infection efficiencies of viruses into cells expressing GFP were set at 100% throughout the study unless stated and the infection efficiencies into GFP-VCA–expressing cells relative to GFP-expressing cells were calculated. For example, when eco HIV-1 was tested, the firefly luciferase activities representing the transfection efficiencies for GFP- and GFP-VCA–transfected cells were 2,065 and 1,854 relative light unit (RLU), respectively, where the background signal was 3 RLU. The renilla luciferease activities reflecting the infection efficiencies into GFP- and GFP-VCA–transfected cells were 4,018 and 1,254 RLU, respectively, where the background was 15 RLU. In this case, the relative infection efficiency of eco HIV-1 into GFP-VCA expressing cells was 34.4%. The relative infection efficiency was introduced because we were able to integrate data from independent experiments. Results from the indicated number of independent experiments were summarized in Figure 1E. Expression of the GFP-VCA significantly reduced the relative infection efficiencies of HIV-1, eco HIV-1, and SIV (30.3, 35.8, and 22.7%, respectively; p 0.01; Figure 1E), whereas those of eco MLV and HSV-1 (98.5 and 103.5%, respectively; Figure 1E) did not. A 10-fold higher or lower titer of HSV-1 did not affect the results (unpublished data). Consistent with this, the average signal-to-noise ratio did not correlate with the efficiency of inhibition (Figure 1E and Table 1). The GFP-VCA did not inhibit eco MLV but did inhibit the infection of eco HIV-1, suggesting that GFP-VCA's ability to inhibit the infection of eco HIV-1 was eco *env*-independent. It also suggested that the cell surface expression of the F10 was not affected by GFP-VCA expression. In addition, our SIV clone did not encode *nef* and HIV-1 *vpr*, demonstrating that both *nef* and *vpr* were not necessary for primate lentiviruses (HIV-1 and SIV) to infect GFP-VCA–expressing cells efficiently. These results suggested that inhibiting the Arp2/3 complex by GFP-VCA negatively affected the infection of primate lentiviruses.

HIV-1 Pseudotyped with VSV-G Overcomes the Block of Infection by GFP-VCA

To gain insight of the mechanism of GFP-VCA's action to limit primate lentiviral infection, we tested whether the GFP-VCA blocked infection of VSV-G–pseudotyped HIV-1 (VSV-G HIV-1). HIV-1 enters cells by inducing the virus-cell membrane fusion at the cell surface. When HIV-1 was pseudotyped with VSV-G, the route of viral entry became endocytosis (Stein *et al.*, 1987; Maddon *et al.*, 1988). We transfected 293 cells with GFP- or GFP-VCA–expressing plasmid along with one-tenth amount of CD4- and F10-expressing plasmids. Then we enriched transfected cells by using magnetic beads directing toward CD4 at 36–42 h posttransfection. This allowed us to measure the infection efficiencies into the transfected cells only (depicted in Figure 2A). More than 90% of the magnetically selected cells were green fluorescence-positive as examined by the flow cytometric analysis (unpublished data). At 48 h posttransfection, cells were infected either with HIV-1, eco HIV-1 or VSV-G HIV-1. For a comparison, amphotropic MLV (ampho MLV) and VSV-G pseudotyped MLV (VSV-G MLV) were tested in parallel. Infected cells were lysed at 2–3 d postinfection, and the virally encoded reporter gene activities were measured to estimate the relative infection efficiencies (depicted in Figure 2A). For example, when eco HIV-1 was tested in parallel with VSV-G HIV-1, the renilla luciferease activities representing the infection efficiencies of eco HIV-1 into mag-

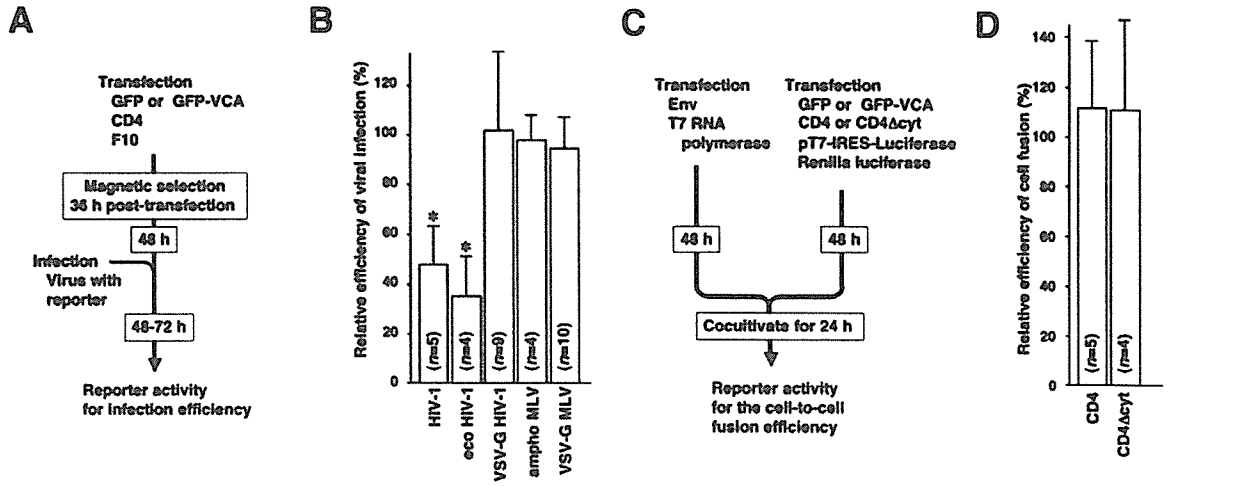

Figure 2. GFP-VCA does not inhibit the infection efficiency of HIV-1 pseudotyped with VSV-G or the membrane fusion induced by the HIV-1's *Env*-CD4 interaction. (A) The experimental procedure using the magnetic selection was drawn schematically. (B) The relative infection efficiencies of HIV-1 and HIV-1 pseudotyped with ecotropic MLV envelope (eco HIV-1) were significantly decreased (asterisk, p 0.01). In contrast, the VSV-G–pseudotyped HIV-1 (VSV-G HIV-1) entered GFP-VCA–expressing cells as efficient as GFP-expressing cells similar to amphotropic MLV (amhpo MLV) and VSV-G–pseudotyped MLV (VSV-G MLV). (C) The experimental procedure for the cell-to-cell fusion assay was drawn schematically. (D) GFP-VCA did not negatively affect the cell-to-cell fusion mediated by HIV-1's *Env* and either the full-length CD4 or the CD4 without the cytoplasmic tail (CD4 cyt) compared with GFP. The data represent the average and SD of indicated number of independent experiments.

netically selected GFP- and GFP-VCA–expressing cells were 41,968 and 10,117 RLU, respectively, where the background was 30 RLU. In contrast, the renilla luciferase activities of VSV-G HIV-1–infected cells were 6346 RLU for GFP-expressing cells and 5436 RLU for GFP-VCA–expressing cells where the background signal was 30 RLU. In these cases, the relative infection efficiencies of eco and VSV-G HIV-1 into GFP-VCA–expressing cells were 24.1 and 85.6%, respectively. Results from a number of independent experiments are summarized in Figure 2B. The relative infection efficiencies for HIV-1 and eco HIV-1 were significantly reduced when target cells expressed GFP-VCA compared with GFP alone (47.3 and 36.0%, p 0.01, respectively; Figure 2B). The magnitude of inhibition of HIV-1 infection in this assay was smaller than that of the first experimental setup (Figure 1D), presumably because the levels of CD4 on the cell surface might have decreased after the magnetic selection (Figure 1E). On the other hand, the relative infection efficiency for eco HIV-1 (36.0%, p 0.01; Figure 2B) was similar to the first experimental setup, indicating that the magnetic selection did not detectably influence the cellular susceptibility to viral infection. Interestingly, VSV-G HIV-1–infected GFP-VCA–positive cells at efficiencies almost equal to GFP-positive cells (101.7%, Figure 2B). Similarly, both ampho MLV- and VSV-G MLV–infected GFP-VCA–expressing cells as efficient as they did GFP-expressing cells (96.9% for ampho MLV, 93.2% for VSV-G MLV; Figure 2B). In this experimental setup, the signal-to-noise ratio of HIV-1 and eco HIV-1 increased compared with the first experimental system; however, the results remained the same (Figures 1E and 2B, and Table 2). These data indicated that the GFP-VCA was unable to block HIV-1 infection when HIV-1 entered cells through the VSV-G–mediated endocytosis. In other words, the reverse transcription, nuclear import, and integration of HIV-1 genome into the host chromosome were able to proceed in the presence of GFP-VCA.

The Efficiency of the Membrane Fusion Is Not Negatively Affected by GFP-VCA

The membrane fusion is the critical event when enveloped viruses infect cells. We next asked if the expression of GFP-

Table 2. Viruses tested in the magnetic selection system

Virus	Virally encoded reporter	Reporter to normalize infection efficiency	Replication-competency	Receptor used in this study	S/N ratio[a]
HIV-1	Renilla luciferase	Firefly luciferase	Incompetent	CD4	7.2
eco HIV-1	Renilla luciferase	Firefly luciferase	Incompetent	F10	101.3
VSV-G HIV-1	Renilla luciferase	Firefly luciferase	Incompetent		251.6
ampho MLV	-galactosidase	Firefly luciferase	Incompetent		12.0
VSV-G MLV	-galactosidase	Firefly luciferase	Incompetent		590.4

See Figure 2.

[a] The signal-to-noise ratio was calculated by dividing the virally encoded reporter gene activities in the GFP-expressing cells by the background signal. Data from all the trials shown in Figure 2 were averaged.

Table 3. Viruses tested in the T7 RNA polymerase system

Virus	Reporter to normalize infection efficiency	Replication-competency	Infected cells harvested (h postinfection)	S/N ratio[a]
IMV	Renillaluciferase	Competent	3	1808.4
Adenovirus	Renillaluciferase	Competent	24	901.3

See Figure 3.

[a] The signal-to-noise ratio was calculated by dividing the luciferase activities in the GFP-expressing cells by the background signal. Data from all the trials shown in Figures 3 and 4 were averaged.

VCA inhibited the membrane fusion through HIV-1's *Env*-receptor interaction. We carried out the cell-to-cell fusion assay in which *Env*-positive cells expressing T7 RNA polymerase (T7RNAP) were fused to the CD4-positive cells carrying the T7RNAP promoter-driven firefly luciferase reporter plasmid (depicted in Figure 2C). The efficiency of the cell-to-cell fusion was measured by the firefly luciferase activity divided by the renilla luciferase activity representing the transfection efficiency. The ratio of the firefly luciferase to renilla luciferase activities in GFP-expressing cells was set at 100%, and the relative efficiencies of cell-to-cell fusion of GFP-VCA–expressing cells were calculated. It revealed that the efficiencies of cell-to-cell fusion initiated by the interaction between HIV-1's *Env* and CD4 were not inhibited when GFP-VCA was expressed in CD4-expressing cells compared with GFP (114%, Figure 2D).

To eliminate a possibility that the GFP-VCA inhibited the expression/distribution of CD4 on the cell surface, we examined whether the CD4 lacking the cytoplasmic domain (CD4 cyt) was able to support the membrane fusion in the presence of GFP-VCA. Because GFP-VCA distributed throughout the cytoplasm, it was unlikely that the motility of CD4 cyt on the cell surface was restricted by GFP-VCA. It was found that CD4 cyt induced the cell-to-cell fusion in the presence of GFP-VCA at efficiencies almost equal to the full length CD4 (113%, Figure 2D). In support of this, enveloped viruses (HSV-1, MLV, and VSV-G HIV-1) were able to infect GFP-VCA–positive cells as efficient as GFP-positive cells (Figures 1E and 2B). In particular, when HSV-1 and ampho MLV enter cells, like HIV-1, the membrane fusion takes place at the cell surface (Fuller and Spear, 1987; McClure *et al.*, 1990; Wittels and Spear, 1991; Nussbaum *et al.*, 1993). These data indicated that the virus-cell membrane fusion was not inhibited by GFP-VCA. According to the data presented hereby, it seemed likely that GFP-VCA did not negatively affect the expression of receptors or viral attachment to receptors, or the virus-cell membrane fusion. Because VSV-G HIV-1–infected cells in the presence of GFP-VCA, we assume that GFP-VCA inhibits HIV-1's life cycle after the membrane fusion before or at the reverse transcription, especially when HIV-1 enters cells through the membrane fusion at cell surface where the viral core is placed in the cortical compartment.

GFP-VCA Inhibits Infection of Intracellular Mature Vaccinia Virus but Not Adenovirus

To test whether the inhibition of viral entry by GFP-VCA was limited to the primate lentiviruses, we examined both intracellular mature vaccinia virus (IMV) and adenovirus. IMV enters cells via the membrane fusion at cell surface, which is accompanied by a drastic actin cytoskeletal reorganization (reviewed by Smith *et al.*, 2002). Adenovirus infects cells through clathrin-dependent endocytosis (Wang *et al.*, 1998). Adenovirus was the only envelope-free virus studied in this article. These viruses encoded T7 RNA polymerase as a reporter (Table 3). To detect the infection signal from transfected/infected cells, we introduced the T7 promoter-driven luciferase reporter into 293 cells (Figure 3A). For example, when IMV was tested, the renilla luciferase activities representing the transfection efficiencies for GFP- and GFP-VCA–transfected cells were 485 and 556 RLU, respectively, where the background signal was 8 RLU. The firefly luciferease activities reflecting the infection efficiencies of virus into GFP- and GFP-VCA–transfected cells were 29,020 and 10,044 RLU, respectively, where the background was 23 RLU. In this case, the relative infection efficiency of IMV into GFP-VCA–expressing cells was 30.3%. Results from a number of independent experiments were summarized in Figure 3B. The relative infection efficiency of IMV was significantly reduced (30.6%, p 0.01; Figure 3B), whereas adenovirus-infected GFP-VCA–expressing cells as efficiently as GFP-expressing cells (98.3%, Figure 3B). IMV gave the highest signal-to-noise ratio throughout the study, yet its infection was blocked efficiently by GFP-VCA (Table 3). Considering all the signal-to-noise data, it was suggested that the signal-to-noise ratio did not positively correlate with the magnitude of inhibition of viral infection. Ten-fold higher or lower titer of either IMV or adenovirus did not affect the results

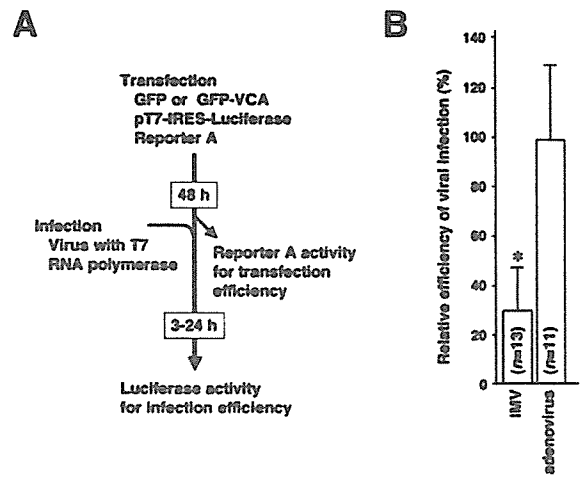

Figure 3. Limiting infection of IMV but not adenovirus by inhibiting the Arp2/3 complex. (A) The experimental procedure was drawn schematically. (B) The significant decrease of relative infection efficiency of IMV, but not adenovirus, was observed (asterisk, p 0.01). The data represent the average and SD of indicated number of independent experiments.

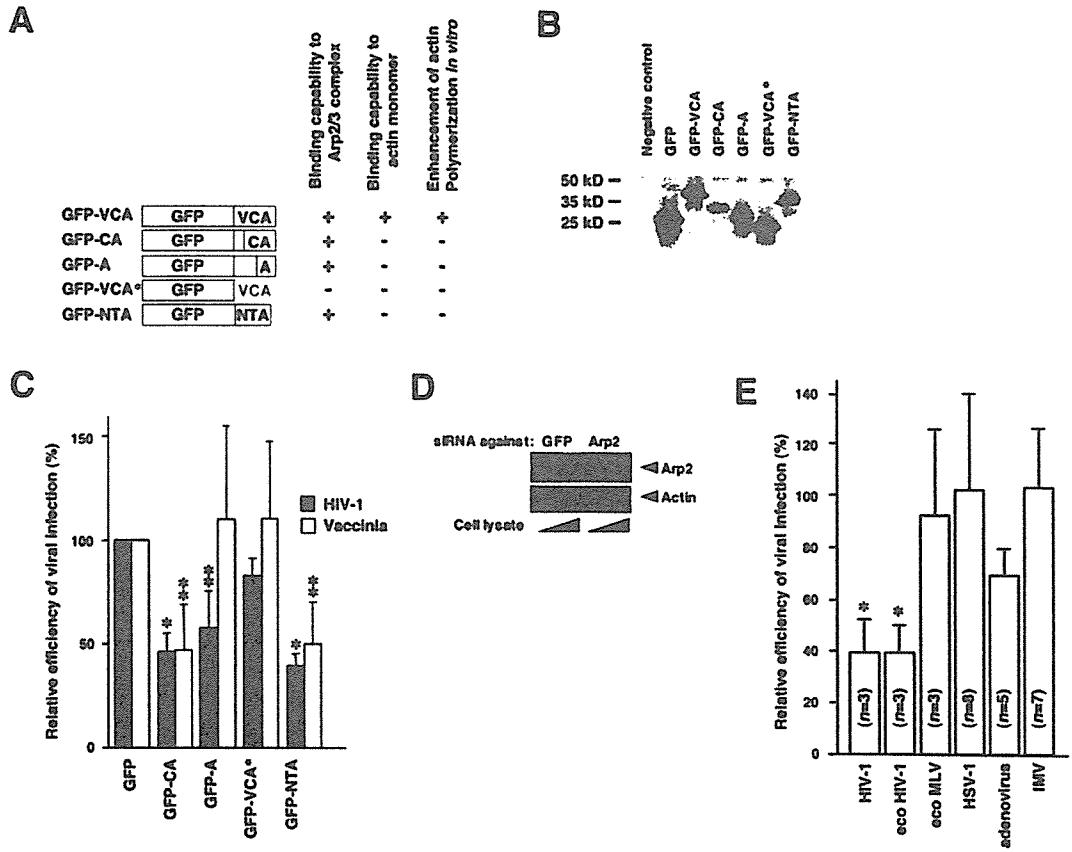

Figure 4. Inhibitory effects of GFP-VCA derivatives, GFP-NTA, and siRNA against Arp2 on the infection of both HIV-1 and IMV. (A) Schematic drawing of GFP-VCA derivatives and GFP-NTA. (B) Western blot analysis detected 30-, 41-, 32-, 30-, 28-, and 37-kDa bands, each predicted mol wt for GFP, GFP-VCA, -CA, -A, VCA*, and -NTA, respectively. (C) The relative infection efficiencies of HIV-1 (■) and IMV ( ) were significantly inhibited when cells expressed GFP-CA and GFP-NTA (asterisk, p 0.01; double asterisks, p 0.05). Expression of GFP-A significantly reduced the relative infection efficiency for HIV-1 but not for IMV. GFP-VCA* did not detectably inhibited infection of both viruses. The data represent the average and SD of more than three independent experiments. (D) The siRNA directed against Arp2 down-modulated expression of Arp2 by 73.5% on the average, whereas the expression of siRNA against GFP did not as demonstrated by Western blot analysis in which 293 cell lysates corresponding to the 5 10^4 or 2 10^5 were analyzed at 2 d posttransfection. (E) Introducing siRNA against Arp2 significantly reduced the relative infection efficiencies of HIV-1 and HIV-1 pseudotyped with ecotropic MLV envelope (eco HIV-1; asterisk, p 0.01) but not ecotropic MLV (eco MLV), HSV-1, adenovirus, and IMV. The data represent the average and SD of indicated number of independent experiments.

(unpublished data). These data suggested that inhibiting the Arp2/3 complex by GFP-VCA negatively affected infection of IMV as well as primate lentiviruses. We focused on HIV-1 and IMV for the further studies.

GFP-VCA's Ability to Nucleate Actin Filament Is Not Necessary to Inhibit Viral Entry

We attempted to locate the domain within VCA responsible for the inhibition of HIV-1 and IMV infection. We generated a series of truncated GFP-VCA mutants (Figure 4A). Their functions were also summarized according to the previous reports (Figure 4A; Takenawa and Miki, 2001; Weaver *et al.*, 2003). Expression of each mutant was verified in Western blot analysis (Figure 4B). Introducing a stop codon into GFP-VCA after the GFP open reading frame allowed VCA-encoding RNA to be expressed but not VCA protein (GFP-VCA*). Expression of GFP-VCA* did not inhibit infection of both HIV-1 and IMV (82.9 and 112.6%, respectively; Figure 4C), suggesting that the inhibition of viral entry attributed to the VCA protein, not the VCA-encoding RNA (Figure 4C). GFP-CA retained the ability to limit both HIV-1 and IMV infection (46.7 and 46.4%, p 0.01 and p 0.05, respectively, Figure 4C). Expression of GFP-A inhibited HIV-1 infection less efficiently than other derivatives (57.7%, p 0.05; Figure 4C). However, GFP-A was unable to limit IMV infection (110.8%, Figure 4C) although synthetic peptides of A subdomain has been shown to retain the binding affinity to the Arp2/3 complex as high as VCA in vitro (Panchal *et al.*, 2003). These data suggested that the V subdomain was not required for the inhibition of HIV-1 and IMV infection. It seemed likely that C and A subdomains functioned cooperatively in vivo to inhibit infection of both HIV-1 and IMV.

To further verify that the reduction of viral infection efficiencies was due to the inhibition of Arp2/3 complex functions, we have tested whether another potential Arp2/3 complex inhibitor NTA, amino-terminal acidic domain of cortactin (amino acids 1–84), was also able to limit both HIV-1 and IMV infection as did VCA. Cortactin is unrelated to WASP family of proteins but is able to bind the Arp2/3 complex through the NTA domain. Expression of GFP-NTA was verified by Western blot analysis (Figure 4B). As expected, GFP-NTA reduced the infection efficiencies of both

HIV-1 and IMV (39 and 50%, p 0.01 and p 0.05, respectively; Figure 4C). These data confirmed that inhibiting functions of the Arp2/3 complex was indeed responsible for limiting both HIV-1 and IMV infection. As GFP-NTA lacked the ability to nucleate actin filaments similar to GFP-CA and because of the reported functions of CA subdomains (Figure 4A), it was strongly suggested that, not their abilities to enhance actin nucleation, but GFP fusion proteins' abilities to bind the Arp2/3 complex was primarily important to inhibit viral infection.

In addition, we tested whether down-regulating expression of Arp2 by using siRNA technique inhibited both HIV-1 and IMV infection. The GFP-VCA and -NTA were able to inhibit functions of Arp2/3 complex by binding to it directly, whereas siRNA against Arp2 down-modulated expression of Arp2, therefore decreasing the number of Arp2/3 complex. Because siRNA against Arp2 was not able to inhibit the function of preexisting Arp2/3 complex directly, it was expected that siRNA against Arp2 should be able to limit viral infection, if any, less efficiently than GFP-VCA. Transfecting the plasmid vector expressing siRNA directing against Arp2 reduced the expression of endogenously expressed Arp2–26.5% in 293 cells as demonstrated by Western blotting analysis (Figure 4D). Viral infection efficiencies were measured using the experimental setups (Figures 1D and 3A) except the GFP or GFP-VCA expression plasmid was replaced with the siRNA expression vectors against GFP or Arp2. When siRNA directing toward GFP was set as 100%, the relative efficiencies of both HIV-1 and eco HIV-1 infection in cells expressing siRNA against Arp2 became 39.4 and 39.1%, respectively (both, p 0.01; Figure 4E). Adenovirus infection was slightly inhibited by the siRNA against Arp2 (69.4%, Figure 4E). However, the relative infection efficiencies of eco MLV, HSV-1, and IMV were not significantly reduced by siRNA directed toward Arp2 (91.3, 103.8, and 104.4%, respectively, Figure 4E). Given that the other two Arp2/3 inhibitors were able to limit IMV and HIV-1 infection, it seemed reasonable to speculate that the inhibition of HIV-1 infection by siRNA was due to the down-modulation of newly synthesized Arp2. However, we were unable to limit the infection of IMV by siRNA against Arp2. We assumed that this was either because siRNA was unable to down-regulate expression of Arp2, therefore Arp2/3 complex, at levels sufficient to block the entry of IMV or the number of the preexisting Arp2/3 complex might be sufficient to support IMV infection, or both.

HIV-1 Replication Is Negatively Affected When GFP-VCA Is Constitutively Expressed in H9 Cells

Finally, we asked whether the replication of HIV-1 was inhibited in T-cells, one of the natural targets of HIV-1. To do this, we isolated H9 cell clones either expressing GFP or GFP-VCA constitutively by infecting H9 cells with MLV vector followed by the limiting dilution. Introducing expression plasmid for GFP-VCA did not alter the morphology of H9 cells compared with GFP-expressing cells or untransfected cells when observed under the confocal microscopy at 48 h posttransfection (Figure 5A) as well as stable cell clones (unpublished data). H9 GFP-VCA clones proliferated at speed indistinguishable from H9 GFP clones (unpublished data). We verified the expression of GFP and GFP-VCA in isolated clones by Western blot analysis (Figure 5B). However, the average expression levels of GFP-VCA appeared low compared with those of GFP in H9 clones (Figure 5B). We infected six H9-GFP and three H9-GFP-VCA clones with a replication-competent HIV-1 (HXB2) and collected culture supernatants at different time points to monitor the viral

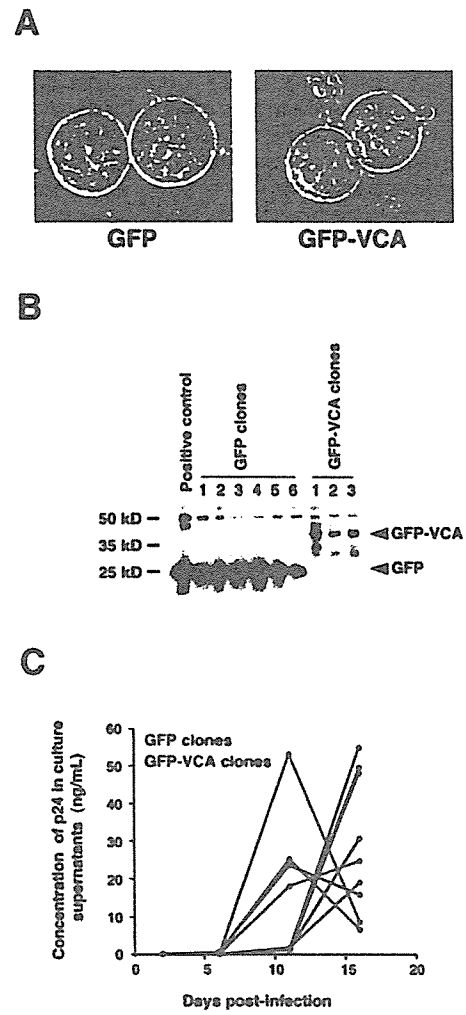

Figure 5. Slow replication kinetics of HIV-1 in H9 cells expressing GFP-VCA constitutively. (A) The morphology of H9 cells was not drastically altered when GFP-VCA was expressed compared with GFP or untransfected cells. The green fluorescent image was merged with the transmission image (magnification, 630). (B) H9 clones stably expressed GFP or GFP-VCA as demonstrated by Western blot analysis (arrowheads). (C) The amount of p24 antigen in the culture supernatants accumulated rapidly in H9-GFP cell clones (red), whereas H9-GFP-VCA clones did not support the efficient HIV-1 replication (blue). Similar results were obtained by two independent experiments.

replication by measuring the amount of p24 viral antigen. The replication kinetics of HIV-1 in GFP-expressing H9 clones showed a rapid propagation of HIV-1 in culture. In contrast, the amount of p24 in the culture supernatants of H9 GFP-VCA clones did not accumulate, suggesting that the HIV-1 replication was substantially suppressed in H9 GFP-VCA clones (Figure 5C). The replication assay was carried out twice consecutively and similar data were obtained. On the average, the peak of HIV-1 replication kinetics in GFP-VCA clones delayed a week compared with GFP clones. The maximum amount of p24 in the culture supernatants of H9 GFP-VCA clones did not appear different from those of H9 GFP clones.

We next examined whether the viruses propagated in H9 GFP-VCA clones were mutants capable of replicating in the presence of GFP-VCA. We isolated viral RNA from the

culture supernatants of a H9 GFP clone and three H9 GFP-VCA clones and sequenced the *gag/pro/pol* region because the GFP-VCA's ability to limit HIV-1 infection did not depend on *Env*, *Nef*, *Vpr*, and *Rev*. However, we could not find any nucleic acid alterations when the viral sequences from an H9 GFP-VCA culture were compared with the one from an H9 GFP culture. These data suggested that the levels of GFP-VCA in H9 clones might be insufficient to confer the selective advantage for mutant viruses to take over the wild-type HIV-1. We found that the late phase of HIV-1 viral life cycle was slightly affected by GFP-VCA. Transfecting proviral DNA into 293 T-cells along with the expression vector for GFP-VCA yielded fewer amount of p24 antigen in the culture supernatant (72%) compared with GFP alone. Taken together, the decreased replication kinetics of HIV-1 in H9 GFP-VCA was assumed to be mostly due to the inhibition of the early phase, partly the late phase, of HIV-1's life cycle. These data demonstrated that the constitutive inhibition of the Arp2/3 complex by expressing GFP-VCA limited efficient replication of HIV-1 in T-cells as well as epithelial cell systems.

DISCUSSION

We have demonstrated that the Arp2/3 complex contributes to the efficient infection of both primate lentiviruses (HIV-1 and SIV) and IMV but not MLV, HSV-1, and adenovirus. Actin cytoskeleton has been shown to play a role in the infection of all the viruses tested in this study according to previous studies using the chemical actin inhibitor (Rosenthal *et al.*, 1985; Kizhatil and Albritton, 1997; Bukrinskaya *et al.*, 1998; Iyengar *et al.*, 1998; Li *et al.*, 1998; Locker *et al.*, 2000). In addition, the Arp2/3 complex-mediated actin nucleation is sensitive to CC (Welch *et al.*, 1998). Therefore, GFP-VCA's ability to limit infection of primate lentiviruses and IMV might be a part of, if not all, the mechanism by which CC reduced the efficiency of viral infection. In other words, primate lentiviruses and IMV might utilize the Arp2/3 complex-dependent actin polymerization system to support their early phase of viral life cycles. In contrast, MLV, HSV-1, and adenovirus might utilize actin to enter cells in an Arp2/3 complex-independent manner. Perhaps, other functional aspects of actin are important for their efficient infection such as the actin cable-dependent trafficking system. Our data clearly demonstrated that the different viruses use actin system differently. It was reported that the infection of HIV-1 was inhibited by CC at least two different levels: 1) by limiting viral receptor/coreceptor clustering upon viral attachment (Iyengar *et al.*, 1998); and 2) by disrupting establishment of active reverse transcription complex (Bukrinskaya *et al.*, 1998). Our findings suggest a possible involvement of the Arp2/3 complex in the latter process or a presence of another actin polymerization-dependent step between two processes.

What is the molecular mechanism by which the Arp2/3 complex supports infection of both primate lentiviruses and IMV? One of the possibilities is that these viruses may activate the Arp2/3 complex and nucleate actin filaments to support their entry. It has been reported that an acidic motif DDW or DEW can be found among cellular Arp2/3 complex-binding proteins including WASP, cortactin, and MyoD as well as *Listeria monocytogenes* surface protein ActA (Weed and Parsons, 2001). We are unable to find such a binding motif in proteins encoded by both HIV-1 and SIV. Therefore, these viruses may not activate Arp2/3 complex due to a direct interaction between viral gene products and Arp2/3 complex. There are two regulatory pathways known to activate the Arp2/3 complex. One is WASP/WAVE pathway and the other being cortactin pathway. Expression of the dominant-negative derivatives of N-WASP, WAVEs, and cortactin were unable to limit the infection of both HIV-1 and IMV (unpublished observation, consistent with the Locker's finding, Locker *et al.*, 2000). The dominant-negative derivative of cdc42, RhoGTPase family protein that locates upstream of WASP/WAVE pathway, was also unable to reduce the relative infection efficiencies of both viruses (unpublished observation). These data implied that the activation of Arp2/3 complex upon infection of both lentiviruses and IMV might be mediated by novel virus-host interactions. Inhibiting the Arp2/3 complex by GFP-VCA did not drastically reduce the efficiency of HIV-1 production as did that of HIV-1 infection, suggesting that the incoming HIV-1 might have something unique which budding virus lacks. We speculate that viral gene products cleaved by HIV-1's protease may be responsible to induce activation of Arp2/3 complex because viral protease become active when viral particles are released from cells such that the cleaved proteins are present at high concentrations only in mature virus particles. VV encodes envelope protein A36R that binds adaptor proteins Nck, Wip, Grb2 that recruits and activates WASP-Arp2/3 complex system (Frischknecht *et al.*, 1999; Rietdorf *et al.*, 2001; Scaplehorn *et al.*, 2002). These molecular interactions are known to be important for vaccinia virus to bud from infected cells as extracellular enveloped virus (EEV). However, IMV does not have A36R on its envelope. Accordingly, IMV should initiate activation of Arp2/3 complex via A36R-independent mechanisms.

On the basis of our data as well as previous observations, we propose models in which the Arp2/3 complex plays a role in the entry of both primate lentiviruses and IMV. HIV-1 enters cells via the membrane fusion on the cell surface (Stein *et al.*, 1987; Maddon *et al.*, 1988). The viral core complex is released to the cytoplasm immediately after the membrane fusion over the cortical layer. Our model is that the viral core components, independent of *Env*, *Nef*, *Vpr*, and *Rev*, recruit adaptor proteins and activate the Arp2/3 complex to generate mechanical force by which HIV-1's core complex passes through the cortical layer and migrates toward the nucleus efficiently (Figure 6A). McDonald *et al.* (2002) had shown that the microtubule system supports long-distance movement of HIV-1's core complex. It is possible that lentiviruses utilize the Arp2/3 complex-mediated active transport system to get access to a subcellular compartment where they meet microtubule system. Consistent with our model, a short-distance rapid movement of HIV-1's core was observed in the time-lapse imaging, which suggested a presence of an actin polymerization-dependent transport (McDonald *et al.*, 2002). On the other hand, IMV enters cells via the membrane fusion at the cell surface as suggested by the intensive studies including electron microscopic studies (reviewed in Smith *et al.*, 2002). IMV infection induces the formation of actin-rich cell surface protrusions partly due to GTPase *Rac1* signaling (Locker *et al.*, 2000) and is inhibited by treating cells with CCD (Vanderplasschen *et al.*, 1998; Locker *et al.*, 2000). Taken together, the Arp2/3 complex-mediated actin polymerization may be required for not only the late phase but also the early phase of IMV's life cycle, specifically at the postmembrane fusion processes (Figure 6B). Also, it is necessary to reorganize the cortical actin network to transport the virus-core toward the cytoplasmic subcompartment where the vaccinia virus replicates. The Arp2/3 complex may play a role in the latter process (Figure 6B). In any case, IMV induces relatively global cytoskeletal reorganization in which a substantial